Role of hemodynamic forces in the regulation of cerebral blood flow

Regulation of cerebrovascular resistance by flow-dependent mechanisms: Implication to normal and pathophysiological conditions

Ph.D. thesis

by

Peter Toth M.D.

Advisor:
Akos Koller M.D., Ph.D.

Program leader:
Samuel Komoly M.D., Ph.D.

Department of Pathophysiology and Gerontology

Doctoral School of Clinical Neuroscience

Medical School, University of Pecs, Pecs, Hungary

2013

"Knowledge is like a sphere, the greater its volume, the larger its contact with the unknown."

Blaise Pascal (1623-1662)

CONTENTS

Part II: Dysfunctional pressure- and flow-induced vasomotor mechanisms in hypertension and aging. Pathophysiological effects on the autoregulation of CBF.

ABBREVIATIONS

CBF: cerebral blood flow

TP receptor: thromboxane/prostaglandin endoperoxide receptor

CVR: cerebrovascular resistance

VCI: vascular cognitive impairment

CBV: cerebal blood volume

α-SMA-GFP: α smooth muscle actin green fluorescent protein

Ang II: Angiotensin II

MCA: middle cerebral artery

HCA: human intracerebral artery

20-HETE: 20-hydroxy-5,8,11,14-eicosatetraenoic acid

HET0016: N-Hydroxy-Ndroxyxytraenoic acidoic aciformamidine

TRPC6: transient receptor potential canonical type channel 6

SKF96365: 1-[2-(4-Methoxyphenyl)-2-[3-(4-methoxyphenyl)propoxy]ethyl]imidazole

BBB: blood-brain barrier

MCP-1: Monocyte chemoattractant protein-1

TNFα: tumor necrosis factor α

IP-10: Interferon gamma-induced protein 10 (also known as C-X-C motif chemokine 10 (CXCL10))

5-NT: 5-nitrotyrosine

Cyp4a12, Cyp4a10, Cyp4a14: cytochrome P 450 4 A family 12, 10, 14

Part I.

Discovering the role of flow-dependent mechanism in the regulation of cerebrovascular resistance. Contribution of hemodynamic forces to autoregulation of cerebral blood flow.

I.1. INTRODUCTION

Regulation of cerebral blood flow (CBF) is of utmost importance to supply the myriad functions of the brain. Many of the mechanisms operating in other organs and tissues are also contributing to the regulation of CBF, however all these mechanisms have to comply with limited space in the closed cranium [1]. Thus maintenance of a relatively constant cerebral blood flow despite of the variations in systemic blood pressure and flow, the so called "autoregulation" of CBF is extremely important and thus, has been always in the center of investigations.

On the basis of an effective autoregulation of CBF it is possible to provide appropriate local changes in blood flow to supply of nutrition and gas for cerebral tissue and serve fluid and gas exchange in the capillaries. Obviously, such a complex function requires complex regulatory mechanisms ensured by the dynamic interaction of mechanotransduction, metabolic (for example adenosine), chemical (such as changes in pCO2, pH and pO2) and other factors, for example, recently there are emerging evidences regarding an important role for glial (astrocytes), pericyte and neural control of CBF [2-15]. In my research I have focused on the novel aspects of the regulation of cerebrovascular resistance and their role in the autoregulation of CBF, because careful analysis of earlier publications and data[5-8, 16-19] revealed that it is unlikely that autoregulation of CBF can be explained solely by the pressure sensitive myogenic mechanism[20-24]. It is of note that the original and perhaps correct definition of "pressure" autoregulation excludes metabolic mechanisms that are thought to contribute to functional hyperemia i.e. increases in blood flow. On the basis of confirming previous findings and discovering a flow-induced vasomotor mechanism, we developed a novel theory/concept for the autoregulation of CBF by hemodynamic forces.

I.1.1. Physiological role of autoregulation of CBF

Total cerebral blood flow has to be relatively constant in order to allow a stable and continuous supply of cerebral tissue and maintain intracranial volume and pressure constant. On the basis of Hagen-Poiseuille law it is assumed that CBF is related to the 4th power of vessel radius, thus an increase in the diameter of vessels elicits an *exponential* increase in blood flow. Therefore in the closed cranium, a general vasodilatation would lead to substantial increase in CBF and cerebral blood volume (CBV) and would lead to elevation of intracranial pressure (and vice versa)[19, 25] which would compress the brain and severely limits its function. Thus, tight control of CBF and CBV is essential for the brain. Indeed, in a wide range of systemic arterial perfusion pressure (from ~ 60 to 140 mmHg) CBF increases only slightly in a *linear* manner measured by different in vivo techniques. [6, 18] At this point it has to be noted, that although in mathematical models gain = 1 is used to indicate so called perfect autoregulation, [22, 23] as also depicted in Figure 1, it is likely that such perfect horizontal relationship does not exist in vivo and it would not be even beneficial to provide an appropriate blood supply of brain tissues. Rather, as Rosenblum suggested, it is likely that the slope increases linearly as pressure and flow increases.[6, 18, 26, 27] Nevertheless, the linear and not exponential (!) increase of CBF in the face of increasing blood pressure is achieved by cerebral autoregulation, although the underlying mechanisms have not yet clarified exactly.

There are some discrepancies in the literature regarding the definition of "autoregulation". Some author include brain tissue metabolism-related mechanisms [3, 6, 14, 15, 28] in the term of "autoregulation" of CBF, which however, should be reserved for explaining the adjusting of blood flow to altered metabolic demands and increased function of neural tissue, i.e. functional hyperemia.[2] Thus in the present work we define autoregulation of CBF to be the result of vasomotor responses to changes in hemodynamic forces achieved by mechanisms intrinsic to the vascular wall, rendering CBF independent from changes in systemic blood pressure, without activating metabolic, chemical, glial, neural and other (for example capillary blood flow regulation by pericytes) regulatory mechanisms. [2, 3, 6-12, 18, 19, 29]

Because changes in pressure are accompanied by changes in flow, in vivo responses of cerebral vessels to changes in hemodynamics are most likely a combination of pressure and flow-induced mechanisms. [30-33] Whereas, the role of changes in pressure has been well investigated in the cerebral circulation, the role of changes in flow eliciting vasomotor

responses received much less attention. In theory, one can hypothesize that changes in flow by eliciting changes in diameter of cerebral vessels contributes to autoregulation of CBF.

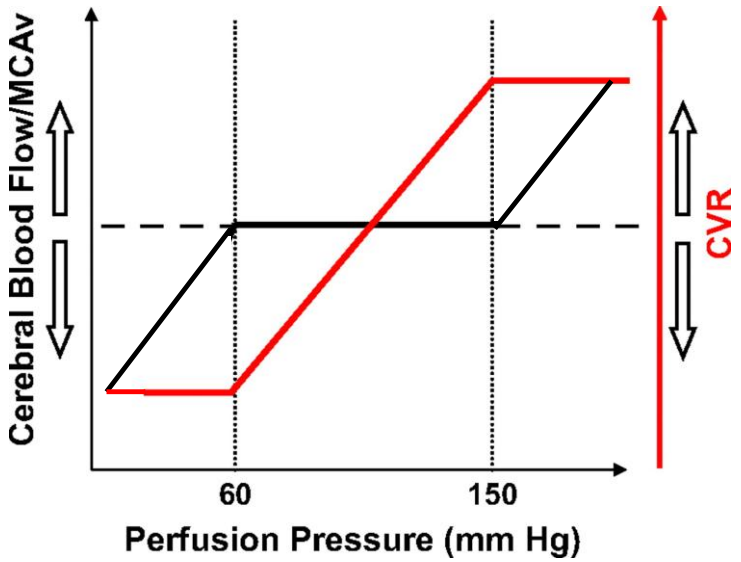

Figure 1. Illustration of the concept of cerebral autoregulation. *Despite of the increase or decrease in perfusion pressure the cerebral blood flow remains constant in a wide range of perfusion pressure by adjusted changes in cerebrovascular resistance (CVR). It has to be noted that in vivo the "plateau" of autoregulation is not perfectly flat, there is a slight increase in CBF as systemic pressure increases. Nevertheless, it is effective enough to prevent an exponential increase of CBF (image from Lucas S J et al. Hypertension 2010;55:698-705).*

Regional and segmental differences in autoregulation of CBF

Importantly, in the cerebral circulation large arteries represent a significant part (≈40 %) of total cerebrovascular resistance. [10, 18, 34-36] In the late 1970's, Kontos at al. investigating the cat pial circulation found that large surface vessels from the circle of Willis to pial arterioles up to 200 micrometers contribute ≈30% of cerebrovascular resistance at 120 mmHg intraluminal pressure and proposed that these vessels are exclusively responsible for autoregulation between 120 and 160 mmHg intraluminal pressure. [18] Similar findings were observed in the rat cerebral circulation. [35] These results showing that in the cerebral circulation both large and small arteries and arterioles take part in regulation of CBF indicated that there might have been a hierarchy in vascular responsiveness, a basis for more precise regulation. This also raised the possibility of spatial characteristics of cerebral autoregulation. Indeed, regional differences were shown in cerebral autoregulatory capacity: hypertension exceeded autoregulation in the cerebrum of the cat (supplied by the internal carotid system), but not in brain stem (supplied by the vertebro-basilar system) demonstrating that autoregulation is more effective in the vasculature of the brain stem. [37-39] In human

cerebral circulation regional differences have also been shown regarding autoregulatory function.[40, 41]

In earlier studies different magnitude of responses in cerebral arteries and arterioles to elevation in pressure were already shown by Kontos et al., [18] and later it was proposed again then demonstrated by Faraci and Heistad at al. that different segmental responses of cerebral vessels to changes in intraluminal pressure underlie the heterogeneity of autoregulation. They demonstrated that pial arteriolar pressure is greater in the brain stem than in the cerebrum implying that pressure drop (and thus resistance) is greater on larger arteries in the cerebrum than in the brain stem. Also, they found that resistance of larger arteries increase in the cerebrum and decrease in the brain stem during moderate increase in blood pressure. They concluded that autoregulation depends primarily on the arterioles in the brain stem, but in the cerebrum larger vessels play an important role. [42, 43] These findings are in line with the findings of Kontos at al. that in the cerebrum larger arteries play a significant part in autoregulation.[18]

In summary, autoregulation ensures that CBF remains relatively constant in a wide range despite of increase or decrease of systemic blood pressure. In vivo, autoregulation of CBF shows regional and segmental differences. In the brain stem (supplied by the vertebro-basilar system) resistance of larger arteries decreases whereas that of arterioles increases in response to elevation in pressure. In contrast, in the cerebrum (supplied by the internal carotid artery system) larger arteries increase their resistance to elevation in pressure greater than the arterioles, playing primary role in autoregulation, and protecting downstream brain circulation from pressure and volume overload. [34, 42, 44]

It is important to note however, that in previous in vivo studies of autoregulation of CBF and underlying cerebrovascular responses the effects of pressure and flow could not be separated and the effect of flow on the diameter of vessels was not even considered. [18, 34, 39, 42, 45-52]

I. 1. 2. Intraluminal pressure-induced responses of cerebral vessels

Earlier findings and new interpretations/conclusions

Until very recently, autoregulation of CBF has been primarily explained by the pressure-induced myogenic response: [44] the inherent property of vascular smooth muscle to dilate to decreases and to constrict to increases in intraluminal pressure. Since its first description by Bayliss, [53] early in the 20th century the myogenic response of different vessels

(arterial, venous and lymphatic) has been widely investigated. In the cerebral circulation it was perhaps first showed by Fog, Forbes and Wolff that pial arterioles of the cat actively dilate and constrict to changes of blood pressure. [9, 54, 55] These findings were confirmed later in studies mentioned above investigating the regulation of CBF, measuring also the simultaneous changes of blood flow, arteriolar pressure etc.

First in the 1980's and since that time, presence of myogenic response has been also shown in vitro in isolated cerebral arteries.[22, 56] In these in vitro studies investigating the myogenic response only pressure was changed, flow was kept constant (this could be done due to the development of novel techniques in which by cannulation of vessel on both ends the intraluminal pressure could be raised by increasing both the inflow and outflow pressure or by closing the outflow end of the vessel and increasing the inflow pressure. In both cases the intraluminal flow remains unchanged. [57-59] Therefore the observed diameter responses were due to changes in pressure alone and were not influenced by changes in flow. As mentioned above we reinvestigated these publications and found that in many of these studies cerebral vessels only maintained a constant diameter between 60-140 mmHg intraluminal pressure. [20-22, 24] This response is referred as the 2nd phase of in vitro arterial myogenic behavior proposed by Osol at al. [21] Interestingly however, if one extrapolated these findings to in vivo conditions it would not achieve autoregulation of CBF. That is, because in the presence of constant diameter, increasing pressure would result in an increased blood flow velocity thus a linear increase in CBF. In contrast, as described above, in vivo measurements of CBF did show that CBF remained relatively constant while intraluminal pressure (and flow velocity) increased! These observations and facts prompted us to hypothesize the existence of a flow sensitive mechanism, which augments the gain of autoregulation close to 1 by eliciting additional constriction.

The strength of myogenic mechanism seems to vary among vascular beds. For example, the myogenic constriction alone likely prevents substantial increases in blood flow during increases in pressure in the cremaster muscle microcirculation.[60] Although, the direct comparison of cerebral vessels to peripheral vessels has to be carried out carefully, Bohlen and Harper [61] and Meininger et al. [62] found that magnitude of myogenic constriction in arterioles of the cremaster muscle is greater than in the comparable sized arterioles of the rat cerebral cortex.

Also, the strength of the myogenic constriction or dilation can be modulated by other factors or conditions. For example, hypertension and exercise can enhance the myogenic response leading to increased constrictions to increases in intraluminal pressure. [22, 61, 63, 64] Also, myogenic dilation can increase significantly under certain conditions. For instance, arterioles in the cat sartorius muscle dilate significantly more to decreases in intraluminal pressure during sympathetic nerve stimulation, enhancing myogenic dilation and providing increased flow. [65]

As we mentioned above, although in many studied cerebral vessels the myogenic response does not reduce the diameter of vessels beyond the basal level in response to elevation of intraluminal pressure, [20-24] it cannot be excluded that magnitude of the myogenic constriction have regional and size differences, and that these vessels possess strong and efficient myogenic responses. At present however, the investigation of myogenic response of microvessels deeply seeded in the brain is technically challenging and the presence of confounding mechanisms in vivo makes it difficult to interpret the findings. The ratio of the magnitude of pressure (and flow-induced) responses in different brain regions and their contribution to cerebral autoregulation should be clarified by future studies.

Molecular mechanisms of the myogenic response of cerebral vessels

Although there are several excellent reviews [66-70] of molecular mechanisms of myogenic response, it would be still appropriate to give a brief overview here.

It is now widely accepted that the primary stimulus to trigger the myogenic response is the pressure-elicited stretch of vascular wall, leading to increased wall tension. [71] However, the sensors are still in question: among others stretch-activated cation channels, Gq-coupled receptors, and interactions between matrix metalloproteinases, extracellular matrix, integrins and the cytoskeleton were proposed.[72-75]

The first event in the mechanotransduction is the depolarization of smooth muscle membrane.[76] Although, there is no consensus regarding the initiators of membrane depolarization, stretch-activated cation channels (TRPC6, TRPM4), calcium-activated potassium channels and chloride channels are probably involved. [77-82] Activation of voltage-gated potassium channels limits depolarization as a negative-feedback mechanism. [83] Depolarization of the membrane then leads to the opening of voltage-gated Ca^{2+} channels (which are also capable to respond to stretch directly [84]) and thus elevated inward Ca^{2+} current. [85, 86] Ca^{2+} can be released from sarcoplasmic stores, as well; however their role in

myogenic response seems to be minor. [84, 87] The increased Ca^{2+} concentration via Ca^{2+}-calmodulin complex leads to myosin light-chain kinase (MLCK) activation. MLCK phosphorylates myosin light chain (MLC_{20}) leading to increased actin-myosin interaction and consequent shortening of smooth muscle cell. [88-90] Because of the circumferential orientation of the smooth muscle cells shortening is translated into constriction of the vessel.

Interestingly, after the initial elevation the intracellular Ca^{2+} concentration does not increase, but the vessel is still constricting. [21] Among others this observation resulted in the discovery of novel Ca^{2+}-independent mechanisms of the myogenic response which can sensitize the constrictor apparatus to Ca^{2+}. As it was mentioned an increased actin-myosin interaction and consequent shortening of smooth muscle cell depends on the phosphorylated state of MLC_{20}, which is governed by myosin light-chain kinase (MLCK) and myosin light-chain phosphatase (MLCP). [70, 91] Ca^{2+}-independent mechanisms altering Ca^{2+} sensitivity of smooth muscle cell act through regulation of MLCP. PKC activation, production of diacylglycerol, RhoA/Rho kinase are involved in these processes. [70, 91-93]

As a second messenger, 20-hydroxyeixosatetraenoic acid (20-HETE) was also found to play a role in myogenic response (also in other vascular beds). [4, 94-96] 20-HETE is capable to inhibit large conductance Ca^{2+}-activated K+ channels and to increase influx of Ca^{2+} via L-type Ca^{2+} channels. [4, 95, 97] Also, one of the major molecular targets of 20-HETE is PKC. [4, 95, 97, 98]

Collectively, there are two critical mechanisms (Ca^{2+}-dependent and independent) contributing to myogenic constriction: 1) increase in pressure via increase in wall tension and smooth muscle cell stretch leads to membrane depolarization, Ca^{2+} influx and constriction via MLCK and phosphorylation of MLC_{20}. 2) In the same time, Ca^{2+}-independent mechanisms involving PKC, diacylglycerol, RhoA/Rho kinase and 20-HETE regulate the activity of MLCP determining the phosphorylated state of MLC_{20} thus sensitizing actin-myosin to Ca^{2+}.

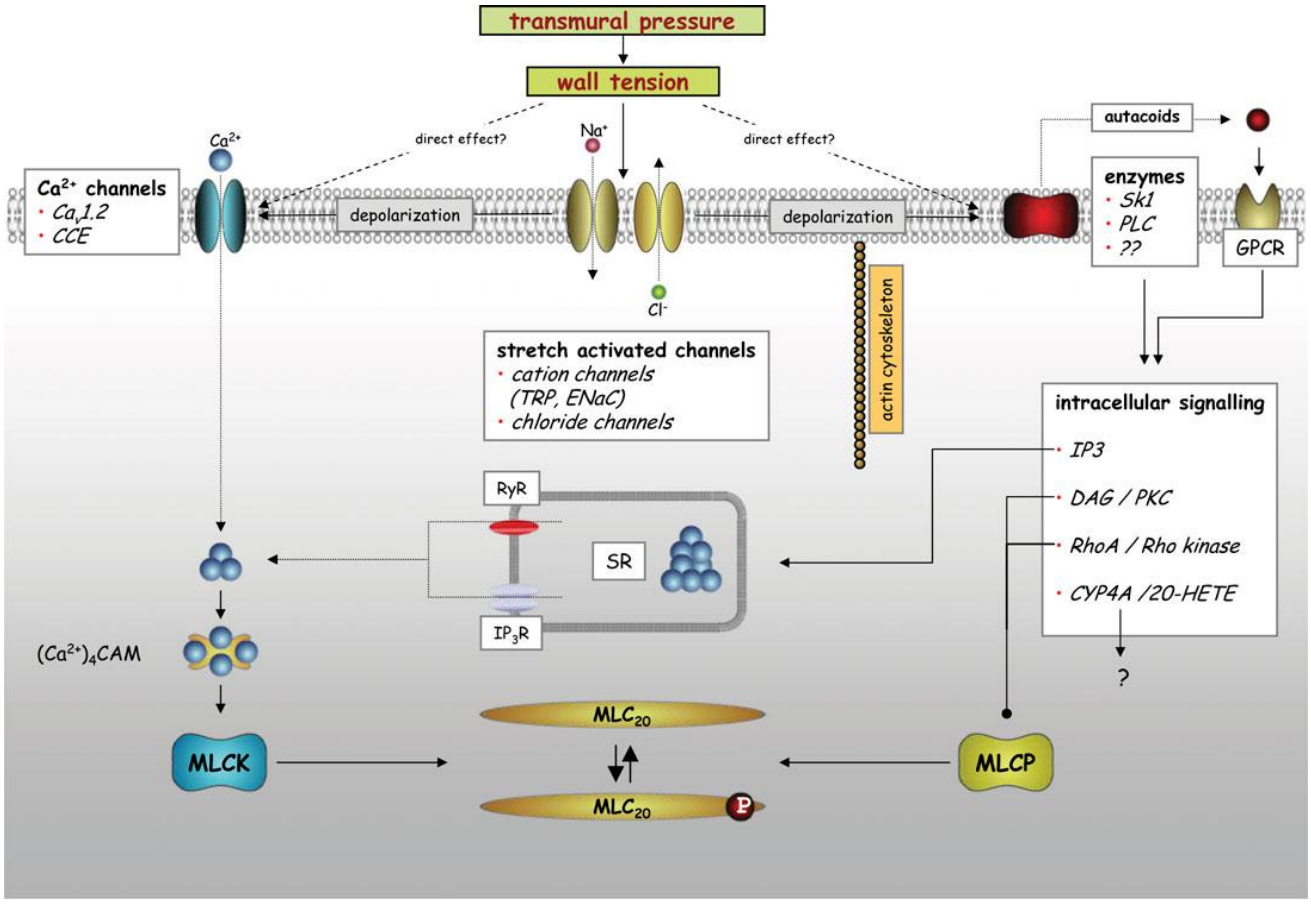

Figure 2. Molecular signaling pathways of the myogenic response. *Increasing transmural pressure activates two main mechanisms responsible for constriction: Ca^{2+}-dependent and Ca^{2+}-independent. For detailed description please refer to the text. TRP –transient receptor protein cation channel, ENaC – degenerin/epithelial sodium cation channel; Cav1.2 – voltage-operated Ca2þ channel; CCE – capacitative calcium entry; (Ca2þ)4CAM – Ca2þ-calmodulin complex; MLCK – myosin light-chain kinase; MLC20 – myosin light-chain regulatory domain (20 kDa); Sk1 – sphingosine-kinase 1; PLC – phospholipase C; GPCR – G-protein-coupled receptor; IP3 – inositol triphosphate; DAG – diacylglycerol; PKC – protein kinase C; IP3R – IP3 receptor; RyR – ryanodine receptor; sER – smooth endoplasmic reticulum; CYP4A – cytochrome P450 4A; MLCP – myosin light-chain phosphatase (from Schubert R at al. Cardiovascular Research (2008) 77, 8–18).*

I.1.3. Flow-induced responses of cerebral vessels

As mentioned above, changes in pressure are accompanied by changes in flow,[30-33] and based on theoretical considerations flow-induced mechanisms may play a role in cerebral autoregulation. Interestingly, there have been only few studies investigating flow-induced

responses of cerebral vessels, which varied between species, vessel types and methods used. [99-104] [105, 106] [107-109]

Constriction of cerebral vessels to increases in flow

In isolated cat middle cerebral arteries Madden at al. found that increases in flow led to decrease in diameter and depolarization of smooth muscle cell membrane.[106] Arteries constricted by flow dilated when PCO_2 was increased, implying that metabolic/chemical signals can override flow-induced constriction. Also, when flow was stopped vessels dilated, and when flow was suddenly increased to the maximal values constriction occurred. Endothelium denudation did not affect flow response, suggesting that flow-induced constriction is endothelium-independent.[106] They also found that administration of integrin-binding peptides, scavenging reactive oxygen species by superoxide dismutase (SOD) and inhibition of tyrosine kinase blocked the constriction suggesting that integrin signaling, free radicals and tyrosine kinase play a role in mediation of flow-induced constriction.

In isolated basilar artery of the Rhesus monkey Sipkema at al. also found flow-induced constriction. However, in many of these earlier studies changes in pressure during changes in flow could not be excluded with great certainty. Therefore in these studies constrictions to flow could be elicited by the activation of myogenic mechanism, as well. Whereas dilation of femoral artery to increases in flow might be caused by flow-induced mechanism, and/or passive dilation (femoral arteries did not develop spontaneous tone). This conclusion is supported by the finding that the active pressure-diameter curves of these vessels did not differ from the passive diameter obtained in calcium free conditions. [110] However, to our best knowledge this is the only study investigating isolated cerebral arteries of monkeys, thus it cannot be excluded that constriction of the basilar artery to flow may be due to species characteristic.

In 2001 Bryan at al. proposed that the controversy and confusion in previous studies were due to different species, different vessel types, different techniques and technical problems causing artifacts, namely the different pH of the extraluminal and intraluminal bath (cerebral vessels are highly sensitive to pH), and the pressure-changes accompanying the increases in flow. Therefore in the same experimental conditions they investigated isolated middle cerebral arteries (MCA), penetrating cerebral arterioles (PA) (≈ 70 μm) and cremaster muscle arterioles (CMA) (which are known to dilate to flow[111]) of rats. They used a syringe pump to generate flow, and decreased the outflow pressure according to the elevation in

pressure due to flow both counted by an algorithm based on the resistance of the tubing and micropipettes and by measuring directly the intraluminal pressure. They made sure that the flow was laminar adjusting the necessary length of the vessel. Maximal flow for PA was 40 µl/min, for MCA 300-500 µl/min. They allowed equilibrating the perfusate before entering the vessel lumen passing it through gas permeable tubing in the extraluminal bath in order to avoid pH differences. In this experimental setup CMA dilated, MCA and PA constricted to increases in flow. The diameter decreased as a function of calculated shear stress, as well (discussed later) [105]. Similarly to Madden at al they observed that an integrin blocker specific for β_3-integrin and SOD abolished the flow-induced constriction. They also measured Ca^{2+} concentration in the vessel wall and demonstrated that flow-induced constriction is accompanied by increases in $[Ca^{2+}]i$. Denudation of the endothelium did not affect flow-induced constriction. [105, 112] Very recently Filosa's group demonstrated flow-induced constriction of rat cerebral arterioles located in brain slices.[113]

Dilation of cerebral vessels to increases in flow

In an *in vivo* study, first Fujii at al. showed that basilar artery of rat dilated when intraluminal blood flow was increased.[114, 115] They used craniotomy to visualize basilar artery. Metabolic parameters (blood O_2 and CO_2, pH) were maintained at a constant physiological level, and blood pressure was kept constant by controlled bleeding of the animal. Blood flow was elevated in the basilar artery by bilateral carotid artery occlusion. It is of note, that among in vivo methods this approach was able to separate the effect of flow and pressure on vessel diameter, while other factors (i.e. metabolic) are controlled. However, what cannot be entirely excluded is that occlusion of the carotid arteries, which decreases blood flow in the carotid system would generate a signal propagating to basilar artery to elicit dilation. Using the same method the group of Sobey confirmed the flow-induced dilation of basilar artery and proposed that it is mediated by H_2O_2 and NO generated by NADPH-oxidase and eNOS, respectively, and PI3-K activation is important in the activation of NADPH-oxidase. [116] In 1993, Gaw and Bevan found also dilation of rabbit cerebral vessels using a wire myograph, [107] in which however flow and pressure cannot be controlled properly. Recently, Drouin at al. demonstrated flow-induced dilation in cerebral arteries. They studied isolated posterior and anterior cerebral arteries of mice in a pressure-flow chamber in a well-controlled manner. [108, 117] They demonstrated, similar to Paravicini at al. that H_2O_2 mediates flow-induced dilation, which however derives from functioning NO-

synthase, activated by an Akt-dependent pathway (Figure 10) [108, 117]. In recent in vitro studies (unpublished observation) we confirmed that in isolated rat basilar arteries increases in flow elicit dilation.

Biphasic response of cerebral vessels to increases in flow

Interestingly, there have been studies, in which biphasic response, dilation and constriction of cerebral vessels to increases in flow was observed. Garcia Roldan and Bevan showed that isolated rabbit pial arteries dilated to 20 µl/min flow at 30 mmHg and they constricted to the same flow at 90 mmHg of intraluminal pressure. [99, 100]

In rabbit cerebral vessels Thorin-Trescases at al. confirmed these findings. They found in secondary and tertiary branches of posterior cerebral arteries that flow induced dilation at 40 mmHg, dilation and a small constriction at 60 mmHg, and a small dilation followed by constriction at 80 mmHg intraluminal pressures. [104] Ward at al. observed similar pressure dependency of flow-induced response of cerebral vessels: in arteriolar branches (≈ 80 µm) of the rat posterior cerebral artery flow elicited dilation at 60 mmHg, and constriction at 120 mmHg intraluminal pressure. [118]

Ngai and Winn studied arteriolar branches of rat middle cerebral arteries (MCA), approximately 35-88 µm in diameter. They achieved increasing flow at a constant (60 mmHg) pressure by changing the inflow and outflow pressure to an equal degree, but opposite direction (the same method developed by us). They also observed that isolated cerebral arterioles, branches of MCA dilated to flow up to 10 µl/min, then restored their diameter at higher flow rates to the initial value. [101]

Similar flow-rate dependency was found by Shimoda at al. Anterior and middle cerebral arteries of the neonatal pig constricted to flow between 0.077-0.212 ml/min, and dilated when flow was raised further (up to 1.6 ml/min). There were no differences in the flow-induced responses at 20 and 60 mmHg intraluminal pressures. In these studies flow was initiated by a syringe pump, and pressure was measured in both the inflow and outflow cannulas by transducers. When flow was raised a micromanipulator decreased the outflow pressure adjacent to the increase in pressure due to flow by sensing the pressure difference between the transducers. The luminal pressure was also measured by inserting a cannula into the lumen of the vessel. [102]

In another study Garcia Roldan and Bevan found the mixture of pressure and flow-rate dependency of flow-induced response of cerebral vessels. In isolated rabbit pial arterioles

they demonstrated that vessels constricted in response to increase in intraluminal flow from 0 to 20 µl/min at 90 mmHg, but did not at the presence of 60 mmHg of intraluminal pressure. Increasing flow up to 100 µl/min constricted vessels at both pressure values.[100] It has to be clear, that biphasic response of diameter to flow does not mean that vessels exhibit opposite responses in a temporal manner, instead it reflects different responses at different pressure values or flow rates.

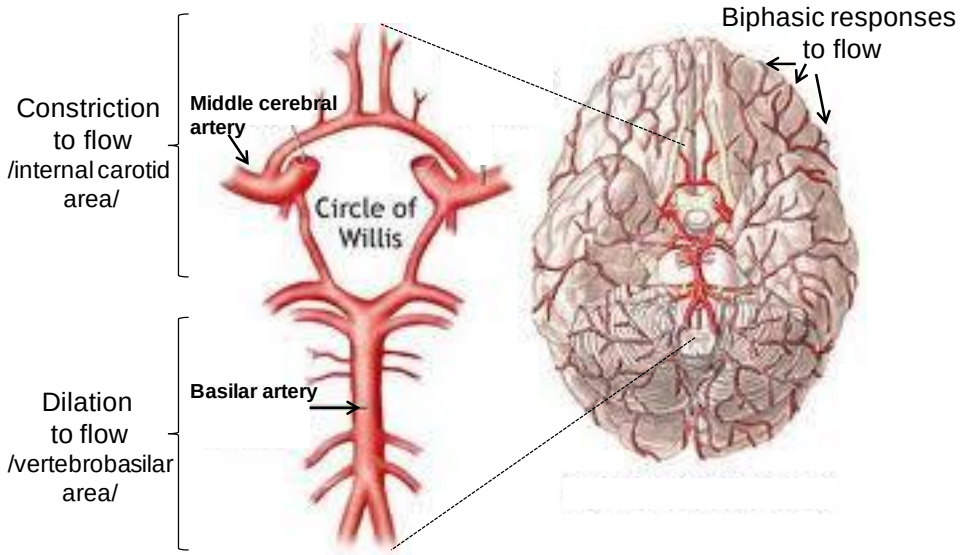

Figure 3. Proposed regional differences in flow-induced responses of cerebral arterial vessels based on literature data*. Studies using a well-controlled methodological approach found dilation to flow in rat and mice in the vertebro-basilar circulatory area; constriction was found in cat and rat isolated cerebral arteries from the internal carotid circulatory area; biphasic responses were observed in rabbit and rat cerebral arterioles showing pressure and flow-rate dependency (dilated at lower and constricted at higher pressure and flow-rates).*

In conclusion, it is not easy to study pressure and flow-induced responses, and the methods and conditions are important to control and consider. Nevertheless, studies using a well-controlled methodological approach found dilation to flow in rat and mice in the vertebro-basilar circulatory area; constriction was found in cat and rat isolated cerebral arteries from the internal carotid circulatory area; biphasic responses were observed in rabbit and rat cerebral arterioles showing pressure and flow-rate dependency (dilated at lower and constricted at higher pressure and flow-rates).

I.2. HYPOTHESIS AND AIMS OF STUDIES

As described above flow-induced responses of cerebral vessels varied between species, vessel types and methods used. [99-104] [105, 106] [107-109] Importantly, no data are available regarding *human cerebral vessels* preventing the translation of knowledge from vertebrates to humans**.** In theory, flow-induced dilation (acting parallel to increase in pressure) would reduce the magnitude of myogenic constriction of cerebral vessels, which would reduce the gain of autoregulation of CBF, whereas if flow elicited constriction, it could contribute to a more efficient autoregulation of CBF. Importantly, the middle cerebral artery supplies those inner areas in which *arteries* have been shown to contribute substantially to vascular resistance controlling blood flow.

Thus, we hypothesized that increases in flow elicit constriction of isolated middle cerebral arteries of rats and intracerebral arteries of humans.

We aimed to assess the potential contribution of flow-induced response of cerebral arteries to the autoregulation of CBF and in a rat model elucidate the underlying molecular mechanisms.

I.3. MATERIALS AND METHODS

Isolation of human intracerebral arteries and rat middle cerebral arteries

All procedures were approved by the institutional animal care and use commeettes of University of Pecs, Medical School, Pecs, Hungary and New York Medical College, Valhalla NY, USA. Studies of human samples were carried out under the approvement of the Regional Ethic and Review Commeette of the University of Pecs.

Human samples

Human brain samples were provided by Prof. Tamas Doczi (Department of Neurosurgery, University of Pecs, Pecs, Hungary) from discarded tissues of patients undergoing neurosurgical treatment of epileptic disorder or cerebral tumors (n=6, age: 32±10 years). [24] The patients did not have any co-morbidity. Preoperative contrast enhanced magnetic resonance imaging (MRI) (for example MP-RAGE sequences) were carefully performed to visualize areas with increased (pathological) blood brain barrier (BBB) permeability. Vessels for the study were selected to be removed from normal, non-enhancing areas that had to be removed due to operative technical reasons to be able to approach deep-seated tumors. In

epilepsy patients areas to be removed were defined by means of MR/CT fusion-based neuronavigation and neither preoperative nor operative cortical electrodes were used. Patients were on only ordinary anticonvulsive medications that directly do not influence microvascular functions. After removal of the brain tissue from the fronto-temporal cortex, it was placed in 0-4 ºC physiological salt solution (PSS) composed of (in mmol/L) 110.0 NaCl, 5.0 KCl, 2.5 $CaCl_2$, 1.0 $MgSO_4$, 1.0 KH_2PO_4, 5.5 glucose, and 24.0 $NaHCO_3$ equilibrated with a gas mixture of 20% O_2 and 5% CO_2, balanced with nitrogen at pH ~7.3.[119] Under an operating microscope, with microsurgical instruments small human cerebral arteries (HCA, 200-300 μm active diameters) were isolated from cortical brain tissue.

Rat samples

Male Wistar-Kyoto rats (250-350 g), fad standard rat chow and free acces to tap water, were anesthetized (intraperitoneal pentobarbital sodium) and decapitated. The brains were immediately removed and placed in PSS. Middle cerebral arteries (MCA) were isolated from both sides of brain of each animal (n=61).

Flow-, pressure-, and simultaneous flow and pressure - induced responses of isolated cerebral arteries

After isolation, cerebral arteries were transferred into a custom made pressure-flow chamber. Inflow and outflow pressures were controlled and measured by a pressure servo-control system (Living Systems Instrumentation, Burlington, VE).

Perfusate flow was measured by a ball flow meter (Omega Inc). The internal diameter was measured by videomicroscopy with a microangiometer (Texas A&M University System). Changes in arterial diameter were continuously recorded digitally by PowerLab system (AD Instruments Ltd) connected to a computer for later analysis. The size of glass pipettes used in this study was matched to both each other and the diameter of the vessels in order to achieve equal resistance.[119, 120] In addition, inflow and outflow reservoirs and position of the chamber were built in a symmetrical manner providing equal pressures or generating flow in the presence of constant pressure in the midsection of vessels.

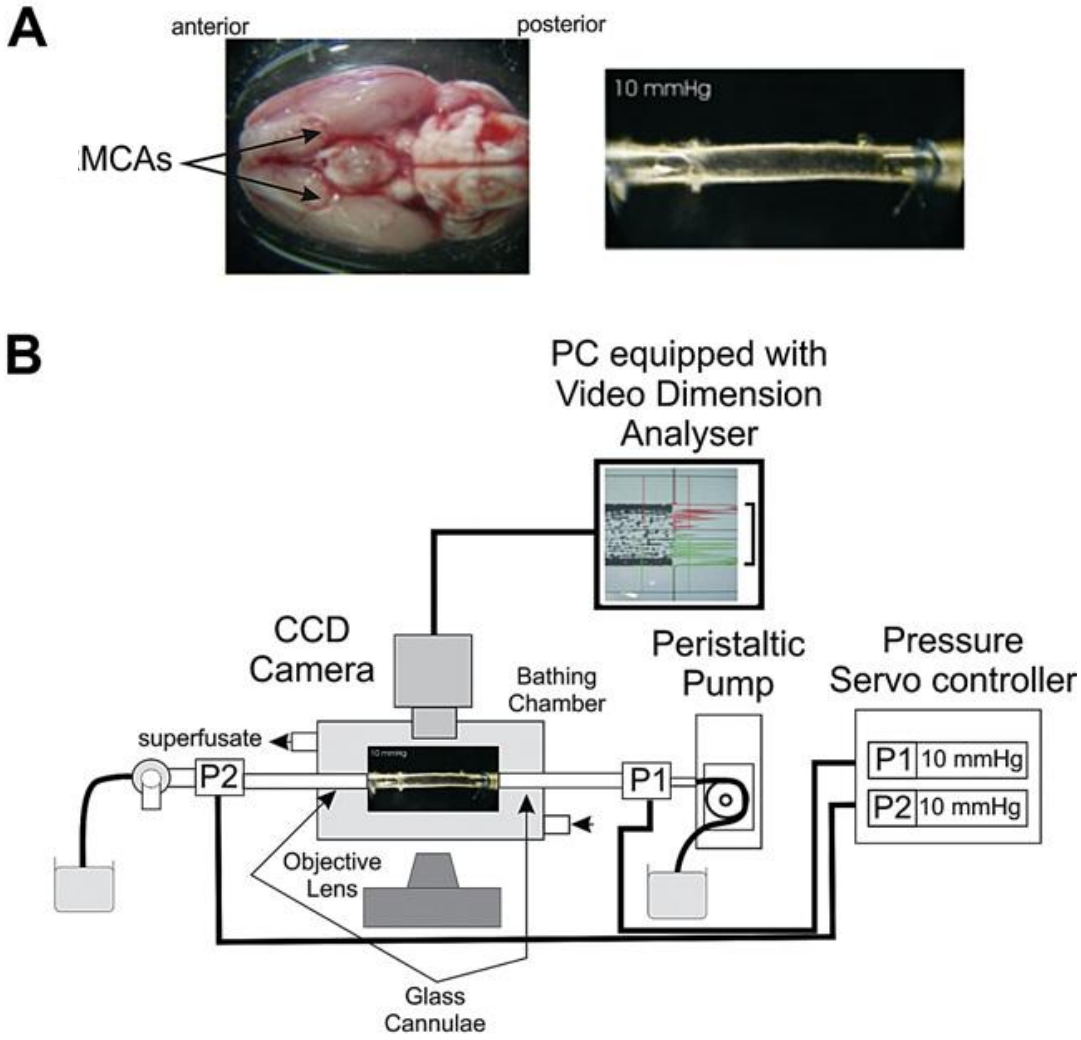

Figure 4. A: *Image of a rat brain showing the origin of middle cerebral arteries (left, MCA) of the rat or mice that are isolated and cannulated by two glass microcannulas in a chamber (right).* ***B:*** *Schematic picture of a pressure/flow myograph system superfused with oxygenated and heated Krebs solution. By changing the inflow and outflow pressure values the intraluminal pressure and flow can be changed separately or simultaneously, and the diameter responses of vessels are measured by videomicroscopy (developed amongst others at New York Medical College, Department of Physiology; the image is based on Cole at al. Archives of Biochemistry and Biophysics 510 (2011) 160–173)*

By the end of the 60 minutes incubation the vessels developed a spontaneous myogenic tone in response to 80 mmHg of intraluminal pressure. First, changes in diameter of cerebral arteries were obtained to stepwise increases in flow elicited by pressure differences (ΔP; established by changing the inflow and outflow pressure to an equal degree, but opposite direction; ΔP = 5, 10, 20, 30, 40 corresponding to 3 to 320 μL/min intraluminal flow. [120] The following general protocol was used: 1) Vessels were exposed to 3 minutes at each flow rate to reach a steady-state diameter. 2) Next, changes in diameter of cerebral

arteries were measured to stepwise increase in intraluminal pressure (0-140 mmHg) in the absence of intraluminal flow by elevating simultaneously the inflow and outflow reservoir to the same level (10 minutes at each pressure step). 3) Then, changes in diameter were measured to stepwise simultaneous increase in pressure and flow. Inflow reservoir was raised from 0 to 140 mmHg and the outflow reservoir was set at 0 mmHg. In a series of experiments the vessels were incubated at flow Δ20 mmHg for 60 min, then flow was decreased to Δ10 mmHg, and then increased to Δ40 mmHg. At the end of each experiment the passive diameters were measured at each intraluminal pressure step in the presence of Ca^{2+}-free PSS containing nifedipine 10^{-5} mol/L.

Theoretical calculations

We have estimated the change in CBF (in arbitrary units) by using diameter values induced by only changes in pressure and then simultaneous changes in pressure and flow using the Hagen–Poiseuille equation ($Q = r^4\Delta P\pi/L8\ \eta$, where Q = flow, r = radius, ΔP = pressure difference, L = length, η : viscosity). We have also calculated a "gain factor (G)" indicating the strength or efficacy of the autoregulation of blood flow used in previous studies.[22] Accordingly, $G = 1-\{[(P_2d_2^4/P_1d_1^4)-1]/[(P_2-P_1)/P_1]\}$, where P: intraluminal pressure, d: diameter, 1 and 2: initial and final pressure values of a pressure step. Thus, G = 1 indicates perfect autoregulation, whereas G<1 means inefficient autoregulation, when flow increases as a function of intraluminal pressure.

Administration of vasoactive agents and enzyme inhibitors

At 80 mmHg intraluminal pressure flow-induced diameter changes of HCA and MCA were repeated in the presence of 20-HETE synthesis inhibitor HET 0016 10^{-6} mol/L [94] for 30 min. Then, flow-induced diameter responses of MCA were repeated in the presence of cyclooxygenase inhibitor indomethacin 2 x 10^{-6} mol/L for 30 minutes, TXA_2 /PGH_2 receptor (TP) blocker SQ 29,548 2 x 10^{-6} mol/L for 30 minutes; free radical scavenger superoxide dismutase-SOD, 200 U/ml for 30 minutes and catalase-CAT, 130 U/ml for 30 minutes; TXA_2-synthase inhibitor ozagrel 10^{-5} mol/L for 30 minutes and. Afterward, 20-HETE (10^{-7} mol/L) was directly administered into the vessel chamber and diameter changes were recorded. In a series of experiments in the presence of Δ40 mmHg adenosine (10^{-5} mol/L) was added into the chamber. The intact vasomotor function of endothelium and smooth muscle was verified by dilation to administration of adenosine triphosphate (ATP) (10^{-5}

mol/L). To test the specificity of HET 0016, acetylcholine-induced (10^{-5} mol/L, n=5) responses were obtained before and after incubation of vessels with HET 0016. All drugs were purchased from Sigma Aldrich Co., except SQ 29,548 and HET 0016 (Cayman Chemical Company).

Expression of CYP450 4A proteins in cerebral vessels

Samples of middle cerebral arteries and gracilis muscle arterioles as control isolated from rats were loaded onto a 10% acrylamide SDS gel and electrophoresed at 100 volts for 3 hours before being transferred to an Immobilon-P nylon membrane (Millipore, Billerica MA). The membrane was blocked in 5% milk/TBS/0.5%Tween for 2 hours at room temperature before the antibody was added and the incubation continued overnight at 4°C. The blots were washed and the secondary antibody was added for 2 hours at room temperature. The primary antibodies included anti-cytochrome P450 (1:4000 dilution, #ab22615, Abcam, Cambridge MA). The blots were washed and a 1:20000 dilution of the anti-rabbit HRP secondary antibody (Amersham, Buckinghamshire, UK) was used. Bands were visualized using a Thermo SuperSignal West Pico kit. Care was taken to ensure that band density remained within the linear range of the film and did not saturate the film, by performing exposures of different times. Band density was quantified using AlphaEaseFC software (AlphaInnotech, San Leando CA).

Detection of Superoxide Level

Superoxide production was assessed in MCA of rat by the dihydroethidium fluorescence method (EB) thought to be specific primarily for superoxide.[121] MCA were isolated from rat brain were placed in a vessels chamber, cannulated, and incubated in the presence of intraluminal flow generated by Δ40mmHg pressure difference in PSS at 37 ºC for 30 min. Some of these experiments were repeated in the presence of HET 0016 10^{-5} mol/L for 60. Control MCAs were incubated in the same conditions in the absence of intraluminal flow. Then, dihydroethidium ($3x10^{-5}$ mol/L) was added to the vials and incubated for 15 minutes. Afterward, MCAs were washed out with PSS and immersed in an embedding medium. Frozen sections of MCAs were visualized by a digital camera attached to a fluorescence microscope (Olympus BX61WI). Intensity of EB fluorescence of the arterial wall was measured and quantified by Image J software. Relative EB fluorescence intensity

was counted by extracting the intensity of the background. Measurement was repeated 5 times, and EB fluorescence was presented as intensity/total area.

Statistical analysis

Statistical analysis was performed by two-way ANOVA followed by a Tukey's post hoc test or Student's t-test. P values less than 0.05 ($p<0.05$) were considered to be significant. Data are expressed as either micrometer or % of passive diameter (maximum diameter of a given vessel in Ca^{2+} free solution is taken as 100%) at corresponding intraluminal pressure and are presented as mean ± SEM.

I.4. RESULTS

Flow-induced responses of cerebral arteries and calculations of CBF

In the presence of constant pressure (80 mmHg) flow elicited by increases in pressure differences caused substantial constrictions of a human intracerebral artery (HCA) (from 246 to 160 μm), as a function of time as shown in an original record in Fig 5. Summary data show that increases in flow elicited significant constrictions of vessels (human: from 74±4.9 to 63±5 %, rat: from 63.8±0.8 to 48.8±1.5 % of passive diameter at 80 mmHg, $p<0.05$). Figure 5 also shows that diameter of MCAs incubated in the presence of flow Δ20mmHg increased when flow was decreased to Δ10 mmHg (to 111±1.7 % of diameter at flow Δ20 mmHg), and decreased when flow was increased to Δ40 mmHg (to 84±1.5 % of diameter at flow Δ20 mmHg). Also, adenosine (10^{-5} mol/L) increased the diameter of MCAs perfused by flow Δ40 mmHg significantly above the baseline diameter (to 148±10 % of diameter at flow Δ20 mmHg).

We found that increases in intraluminal pressure decreased normalized diameter of MCA (from 84±3 to 53±4 %, n=6), whereas simultaneous increase of pressure+flow enhanced the only pressure-induced decrease in diameter (from 83.8±3 to 36±3 %, $p<0.05$) (Fig 7). When only pressure was increased eCBF showed a linear increase from 1.4±0.1 to 23.3±7.6 in arbitrary units. In contrast, when pressure+flow increased simultaneously first the eCBF decreased significantly to 0.7±0.1 and then increased only to 5.4±1.4 in arbitrary unit (Fig 6).The gain of autoregulation (G) calculated using diameters induced by pressure alone was 0.8±0.1, whereas G was 0.99±0.1 when pressure+flow were increased simultaneously.

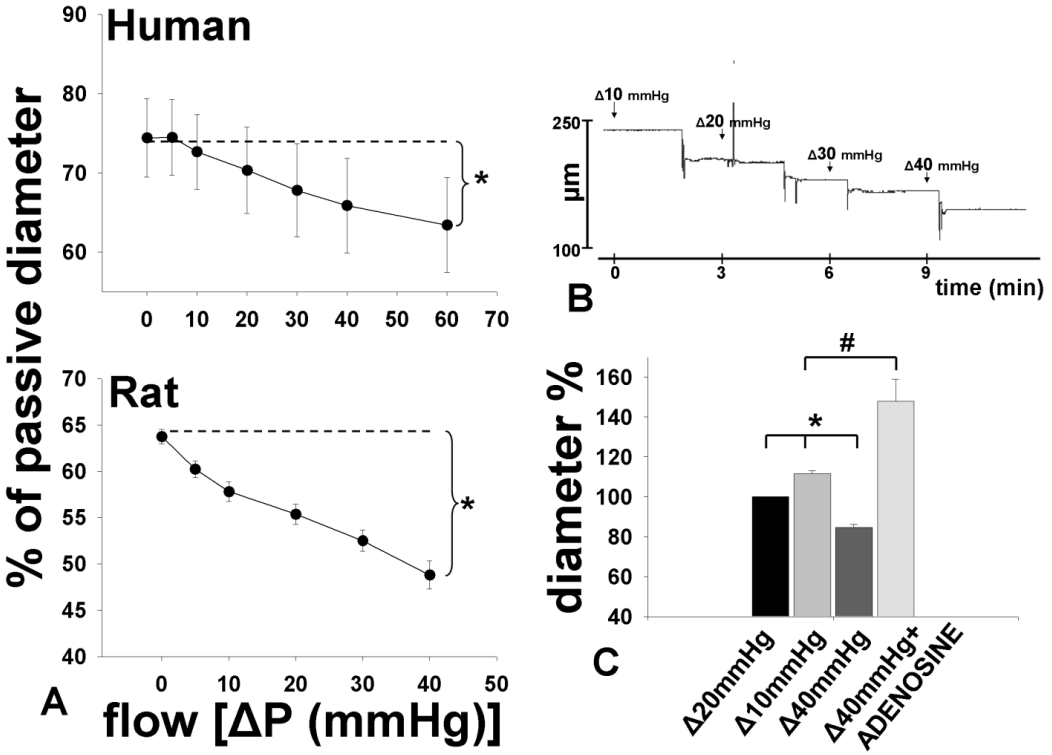

Figure 5. A: *Changes of diameter of human cerebral arteries (n=6) and rat middle cerebral arteries (n=12) as a function of intraluminal flow indicated as [ΔP(mmHg)].* ***B:*** *Original record of diameter (μm) of a human cerebral artery to increases in intraluminal flow (ΔP=10, 20, 30 and 40 mmHg) as a function of time (min).* ***C:*** *Diameter changes of rat middle cerebral arteries (n=6) perfused by flow Δ20 mmHg to decreased flow (Δ10 mmHg) and increased flow (Δ40 mmHg), and to administration of adenosine (10^{-5} mol/L) in the presence of flow Δ40 mmHg. Data are mean ± SEM (*, # p<0.05).*

Mechanism of flow-induced response of cerebral arteries

Summary data show, that incubation of the vessels with HET0016 (inhibitor of 20-HETE production by blocking Cyp4504A enzymes) abolished the decrease in diameter of both HCA and MCA elicited by increases in flow (Fig 7). Direct administration of CYP 450 metabolite 20-HETE (10^{-7} mol/L) decreased the diameter of MCA similarly to flow (at ΔP=40mmHg, flow:42±3, 20-HETE: 34±9.8 Δμm) (Fig 7).

Dilations of MCA in response to ACh were not affected significantly by HET 0016 (before: 53±4.6 % after: 46±5.4 % of maximal dilation). Fig 7 shows that cytochrome P450 4A enzymes are present in the MCA of rat.

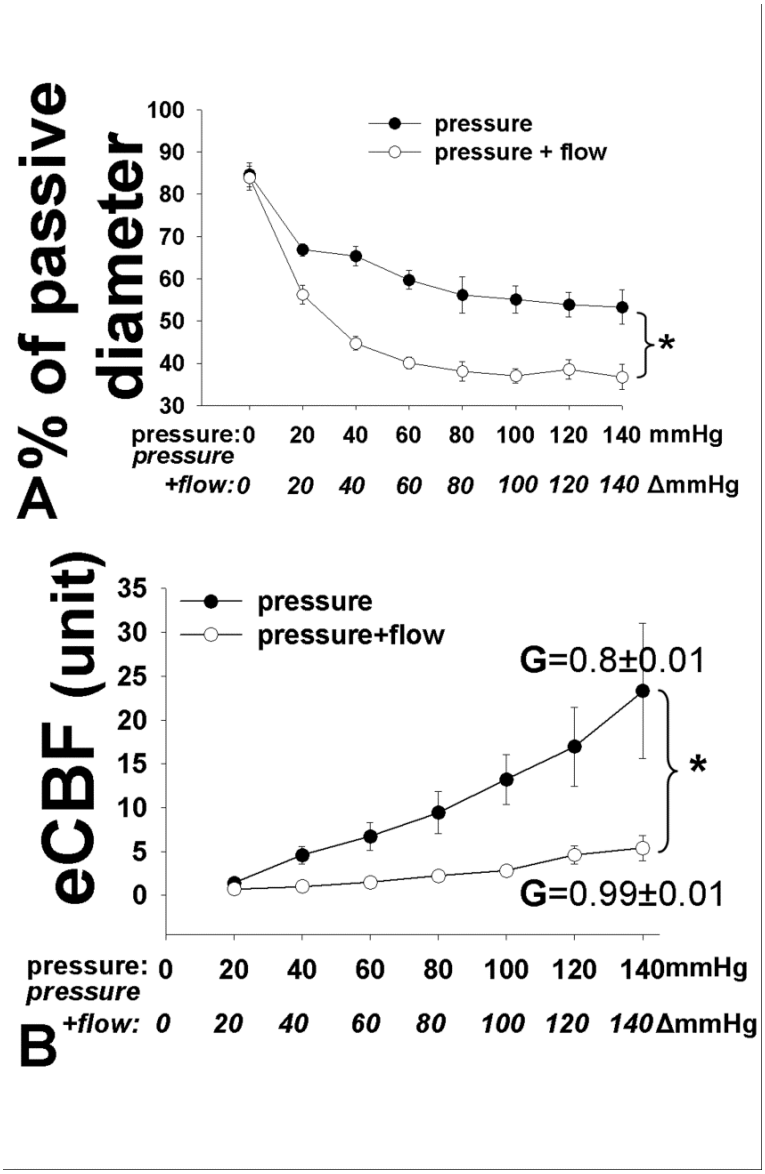

Figure 6. A: *Summary data of normalized diameter changes of rat middle cerebral arteries (n=6) as a function of intraluminal pressure (mmHg) and pressure plus flow (ΔmmHg).* ***B:*** *Changes of extrapolated CBF (eCBF) in arbitrary units (unit) as a function of pressure (mmHg) and pressure+flow (ΔmmHg). Calculated gain (G) of CBF was 0.8±0.1 when pressure was raised, and increased to 0.99±0.1 when pressure + flow were raised. Data are mean ± SEM (*p<0.05).*

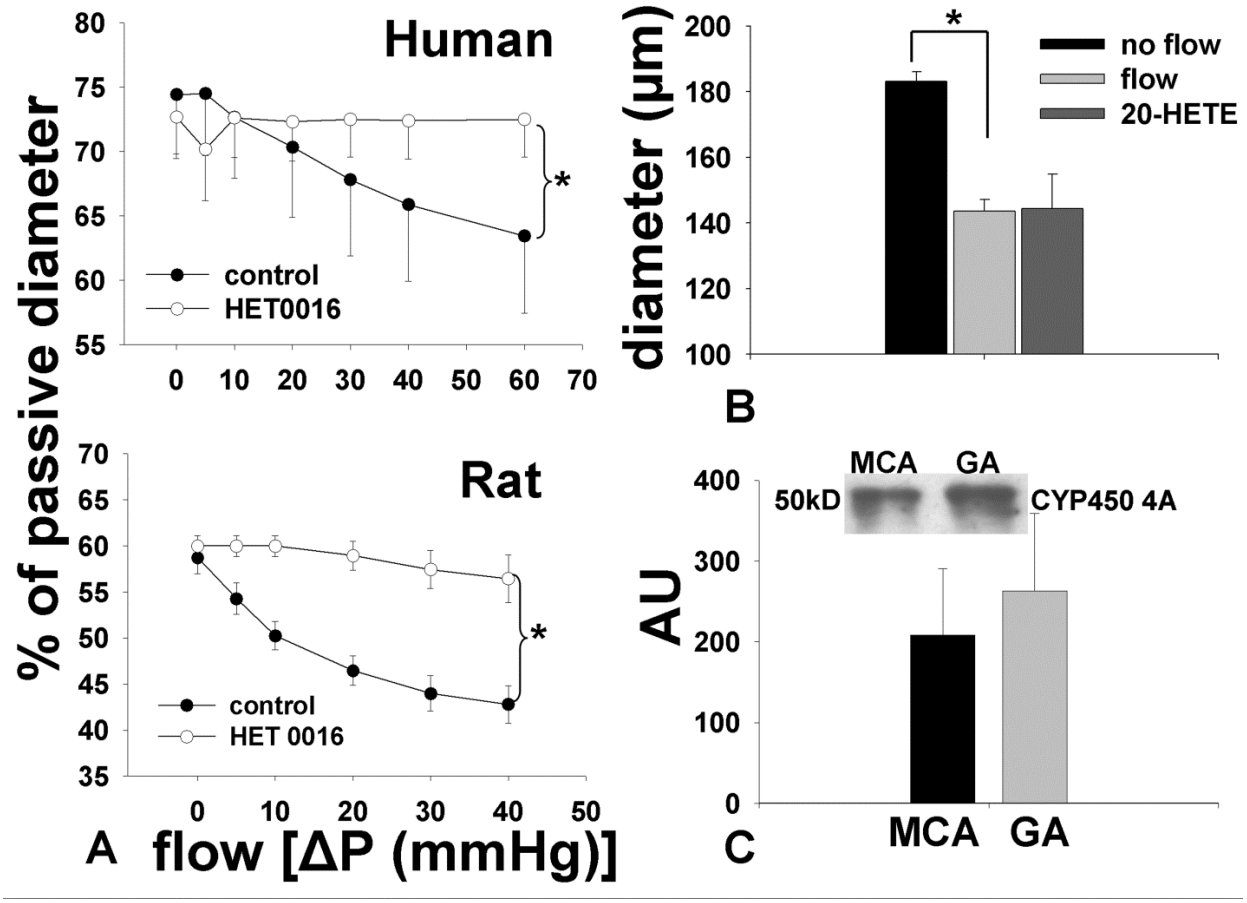

Figure 7. *(**A**) Diameter changes (as % of passive diameter) of human intracerebral arteries (n=6) and rat middle cerebral arteries (n=6) as a function of intraluminal flow [ΔP(mm Hg)] in the presence of 20-hydroxyeicosatetraenoic acid (20-HETE) synthesis inhibitor HET0016 (10^{-6} mol/L). (**B**) Summary data of diameter changes (μm) of rat middle cerebral arteries (n=4) to increased intraluminal flow (ΔP=40 mm Hg), and to direct administration of 20-HETE (10^{-7} mol/L). (**C**) Expression of cytochrome P450 4A protein (CYP450 4A) in middle cerebral arteries (MCAs) and gracilis arterioles (GA; as control; n=4). Integrated density value is expressed as arbitrary unit (AU). Data are mean±s.e.m. ($^{*}P<0.05$).*

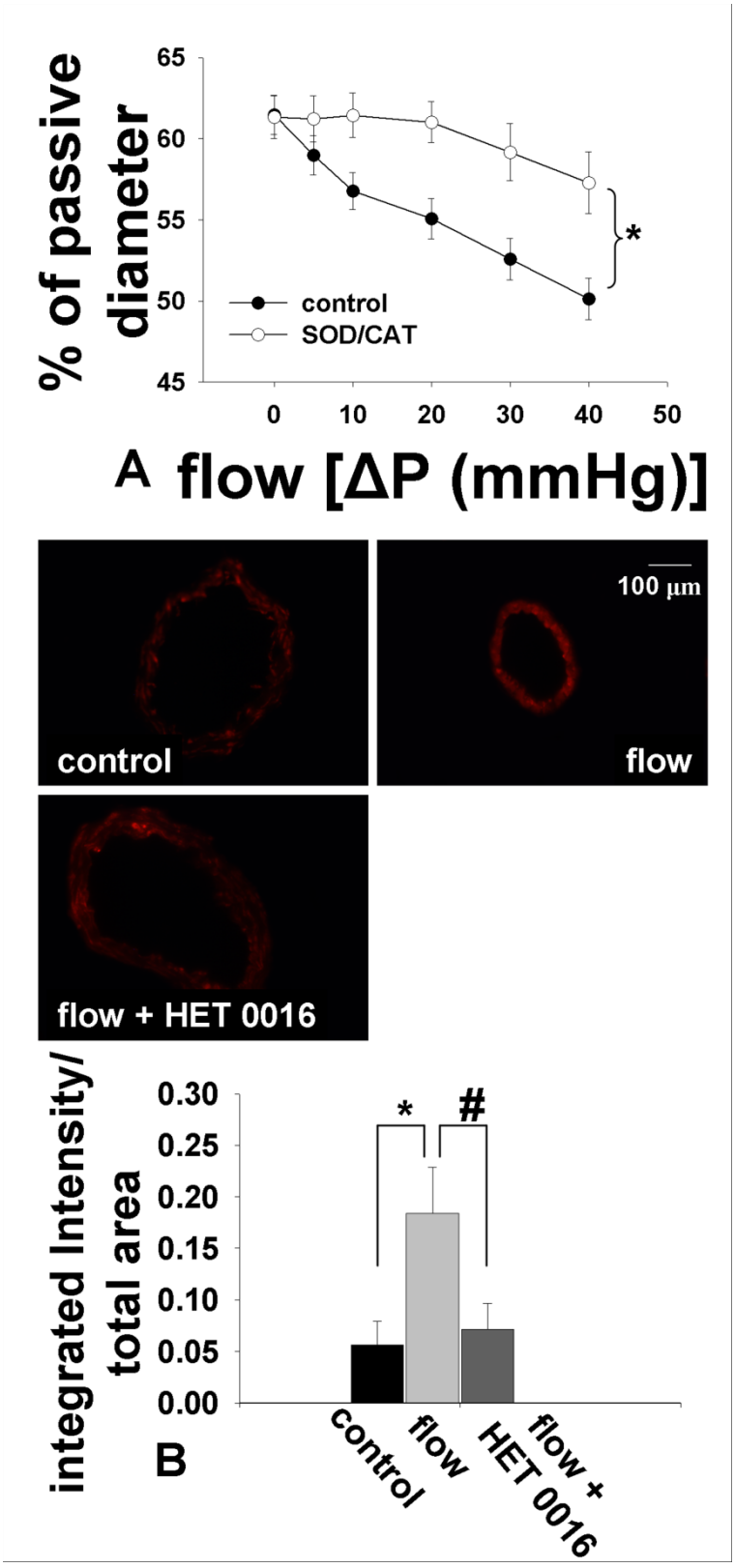

Figure 8. *(**A**) Diameter changes of rat middle cerebral arteries (n=6) as a function of intraluminal flow in the presence of superoxide scavenger superoxide dismutase plus catalase (**B**) Representative pictures and summary data of ethidium bromide (EB) fluorescence of sections of middle cerebral arteries of rat in the absence (control) and presence of flow (flow), generated by Δ40 mm Hg pressure difference, and in the presence flow and 20-hydroxyeicosatetraenoic acid synthesis (cytochrome P450 4A) inhibitor HET0016 (10^{-6} mol/L) (flow+HET0016). Data are mean±SEM. ($^{*,\#}P<0.05$).*

Incubation of vessels with SOD/CAT significantly decreased the reduction in diameter of rat cerebral arteries elicited by increases in flow. Representative EB fluorescent images of sections of MCA and summary data demonstrate an enhanced EB fluorescence in the vessels exposed to flow compared to control (absence of flow). Enhanced EB fluorescence was reduced to the control level by HET 0016 (10^{-5} m/L) (control: 0.05±0.02, flow: 0.18±0.04, flow+HET 0016: 0.07±0.02 integrated intensity/total area, respectively; $p<0.05$) (Fig 8).
Summary data show that incubation of the vessels with indomethacin or SQ 29,548 inhibited the constriction of MCA to increases in flow, whereas ozagrel did not have an effect (data not shown).

I.5. DISCUSSION OF FINDINGS

***Physiological significance of flow-induced responses of cerebral vessels. Developing a novel concept for the autoregulation of CBF*.**

The present study established that increases in flow elicit constrictions in the isolated middle cerebral arteries of rats and isolated cerebral arteries of humans. These findings can have major impact on our understanding of the autoregulation of CBF, because previously only the pressure-induced myogenic response was used to explain autoregulation of CBF, which however, seems to be inefficient on its own.

From the observed responses of cerebral vessels one can estimate the change in CBF by using diameter values induced by only changes in intraluminal pressure and then simultaneous changes in pressure and flow using the Hagen–Poiseuille equation. [23] Also, a "gain factor (G)" can be calculated indicating the strength or efficacy of the autoregulation of blood flow (G = 1 indicates perfect autoregulation, whereas G<1 means inefficient autoregulation, when CBF increases as a function of intraluminal pressure). [22, 23] In case of flow-induced constriction we found that simultaneous increase of pressure+flow enhanced the only pressure-induced decrease in diameter. Also, the gain of autoregulation (G) calculated using diameters induced by pressure alone was below 1, whereas G was ≈1 when pressure+flow were increased simultaneously indicating a more efficient autoregulation. When only pressure was increased estimated CBF showed a linear increase, but when pressure+flow increased simultaneously estimated CBF decreased significantly and remained relatively constant. [23] Based on this we propose that in the vascular networks where vessels

constrict to flow simultaneous operation of pressure- and flow-induced constrictions is necessary to explain an effective autoregulation of CBF (Figure 9).

In the cerebrum, in the internal carotid circulatory system resistance is profoundly determined by larger arteries.[18, 34, 35, 42] In line with this, larger arteries (i.e MCA) constrict to increases in flow, which enhances the pressure-induced tone of cerebral vessels leading to a more efficient autoregulation of CBF, and this way, flow-induced constriction of cerebral arteries plays an important role in regulating cerebral blood volume and intracranial pressure. Therefore, in addition to myogenic response, flow-induced constriction may also participate in the development of segmental resistance of the cerebral circulation, because both large arteries and arterioles respond to changes in flow with either constriction or dilation. [23, 99-101, 105, 108, 114, 122]

Regarding flow-induced responses the importance of segmental function of cerebrovascular resistance and the role of large arteries are underlined by the findings of Fujii at al. and Garcia-Roldan and Bevan [99, 101] showing that isolated cerebral arterioles (downstream from arteries) constricted when pressure or flow rate is high and dilated when they are low. Thus these mechanisms protect downstream brain circulation from pressure and volume overload. [34, 42, 44]

Importantly, the vasomotor tone "set" by the two hemodynamic forces can be modulated or overridden by other factors sensitive to the needs of neural tissues. That is blood flow still can be altered locally (for example due to metabolic factors) during increased demand. Such as, local neural needs can increase cerebral blood flow regionally via neural, glial and other regulatory mechanisms, which can also be propagated to upstream vessels. [2, 17, 123] This concept is in line with the suggestion of studies showing that metabolic dilation could overcome the constrictor effect of pressure or flow. [23, 106, 124, 125] Conversely, in the brain stem (vertebro-basilar system) arterioles are the major site of resistance, [42, 43] thus larger arteries, such as the basilar artery "can" dilate to flow participating in reactive hyperemia. [122]

The heterogeneity of autoregulation is likely due to the different efficacy of pressure and flow sensitive vascular mechanisms and/or different magnitude of contribution of metabolic mechanisms and neurovascular coupling. The proposed concept should be further clarified in the future by in vitro investigation and comparison of pressure- and flow-induced responses of cerebral arteries and arterioles from different regions of cerebrovascular tree. [126] More importantly, in vivo imaging of CBF in experimental animals and humans could be performed by means of MRI, laser speckle imaging and other novel techniques in order to

clarify the mentioned concept of the role of hemodynamic forces in regulation of CBF, in which pharmacological intervention of signaling mechanisms may reveal further detail of autoregulation of CBF.

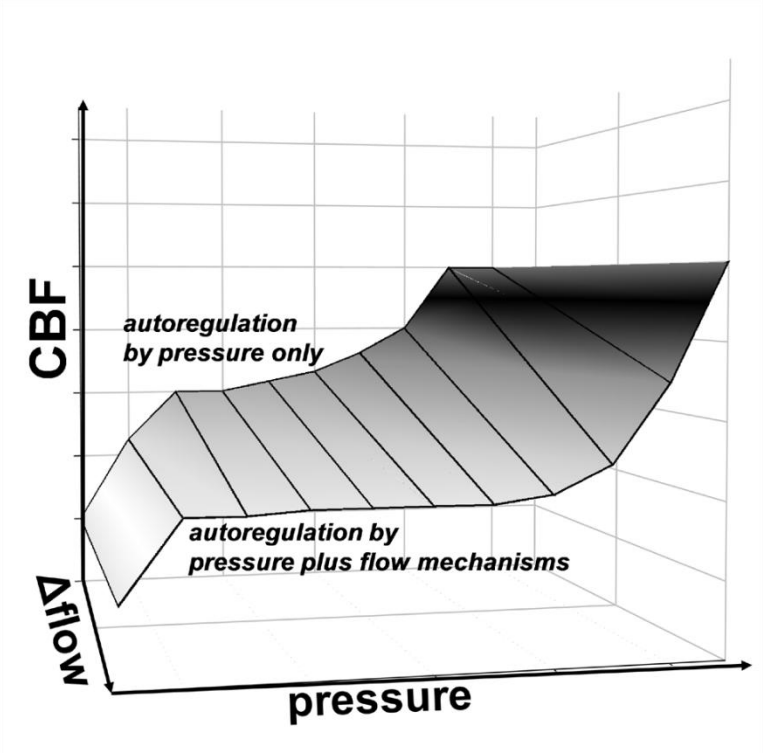

Figure 9. Proposed physiological role of flow-induced constriction of cerebral arteries in autoregulation of cerebral blood flow. *Combined effect of intraluminal pressure and intraluminal flow (Δ flow) achieves effective autoregulation of cerebral blood flow (CBF), while only pressure-induced diameter responses lead to increases in CBF, thus inefficient autoregulation.*

Signaling mechanisms responsible for mediating flow-induced constriction of cerebral arteries

Arachidonic acid and its metabolites (such as CYP450 4A derived 20-HETE, COX derived TXA_2,) play major roles in the regulation of cerebrovascular resistance. [94, 127, 128] Harder and Gebremedhin at al. and others showed that AA is metabolized by cytochrome P450 ω-hydroxylases (CYP450 4A) into 20-hydroxyeicosatetraenoic acid (20-HETE) [4, 95] and it plays important role in the regulation of cerebrovascular tone, by mediating agonists- and pressure-induced constrictions of vascular smooth muscle of cerebral vessels. [94, 129] Thus it seemed to be logical to hypothesize that 20-HETE could be the constrictor factor mediating the flow-induced constriction of cerebral arteries, as well. Indeed, we found that flow-induced constrictions of human cerebral arteries and MCA of rat were abolished by

administration of HET 0016 (Fig 7.), an inhibitor of 20-HETE production. Consistently to these functional findings we found that CYP450 4A enzymes are present in the MCA of the rat, a finding similar to that of Gebremedhin and Dunn at al. [94, 128]

It is also known, that production and direct administration of 20-HETE by cytochrome P450 can produce ROS.[106, 112, 130] In the present studies we found that administration of ROS scavengers significantly reduced the flow-induced constriction of cerebral arteries (Fig 8). In addition, our findings showed increased EB fluorescence in MCA after exposing the vessels to flow, suggesting flow-induced increased ROS production. The enhanced production of ROS was reversed by inhibition of 20-HETE production (Fig 8), suggesting ROS is generated during synthesis of 20-HETE, which is elicited by increases in flow. These findings demonstrate that ROS are generated during flow-induced activation of CYP450 4A, [130] but because HET 0016 abolished flow-induced constriction, ROS unlikely have major direct vasomotor effect in this condition.

Previous studies[131, 132] have proposed that 20-HETE constricts cerebral arteries by various pathways. For example, 20-HETE activates protein kinase C (PKC), depolarizes smooth muscle cells by inhibition of large-conductance K_{Ca} channel, and increases Ca^{2+} influx via L-type Ca^{2+} channels. In addition, thromboxane A_2 is another constrictor metabolite of AA and known to have a profound effect on cerebrovascular tone. [127] Thus we evaluated the effect of TXA_2 synthase inhibitor ozagrel, and TP receptor blocker SQ 29,548. Importantly, SQ 29548 abolished the flow-induced constriction, but ozagrel did not have any effects (data not shown).

Our results that both inhibition of 20-HETE production and antagonizing TP receptor abolished flow-induced constriction suggest that 20-HETE acts on TP receptor. Consistently with this hypothesis previous studies [133, 134] by Schwartzman at al. proposed that 20-HETE caused constriction of arteries via TP receptor after 20-HETE was metabolized by COX into 20-endoperoxides (20-OH-PGH_2, 20-OH-PGG_2). This finding is supported by our finding that indomethacin also blocked flow-induced constrictions of MCA. The proposed molecular mechanisms mediating flow-induced constriction of human and rat cerebral arteries are summarized in Fig 10.

Interestingly, in vivo application of ROS caused dilation of pial arterioles and systemic administration of scavengers of ROS or inhibition of COXs reduced or did not affect CBF. [135-137] These findings could be due to the fact that multiple sources of ROS and COXs are present in the cerebral vessels and in the surrounding neural tissues and astrocytes, [138]

releasing both constrictor and dilator factors. [139, 140] Thus, in vivo administration of drugs generating or inhibiting ROS production could activate several opposing vasomotor mechanisms. Also, to ensure appropriate blood flow to cerebral tissues several multilevel, confounding mechanisms are present. Thus *in vivo* the lack of or inhibition of one mechanism activates compensatory mechanisms to maintain CBF.

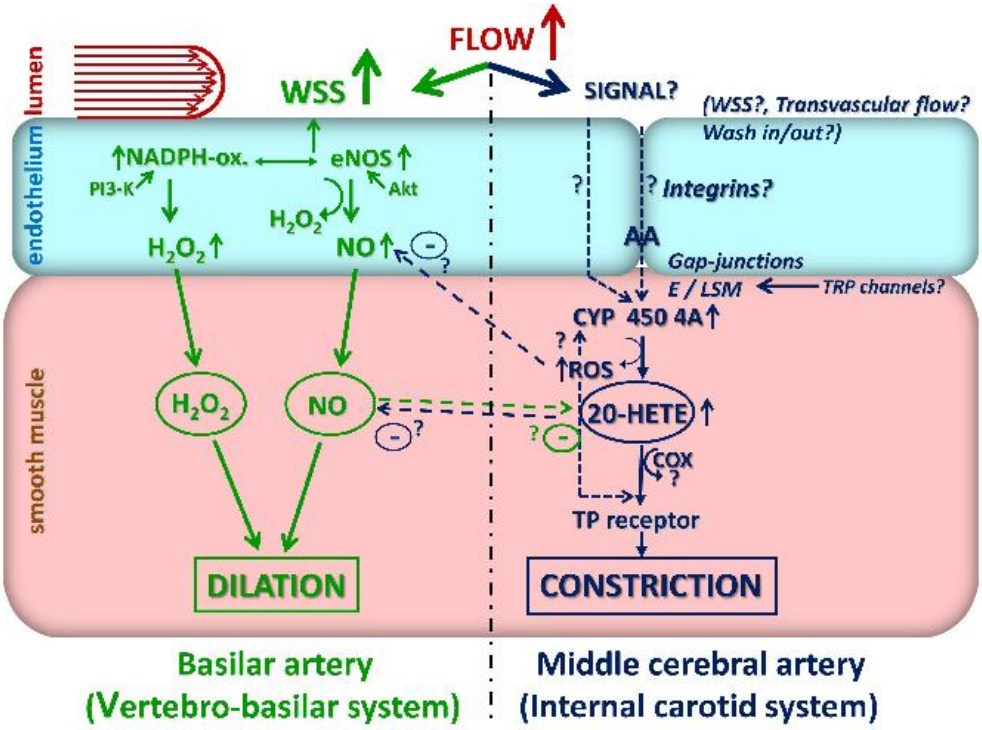

Figure 10. *Flow induces dilation, biphasic responses, or constriction of cerebral vessels depending on the regional and segmental localization of the vessels. We propose that in the internal carotid system larger arteries (such as the middle cerebral artery) constrict to increases in flow. The flow-induced constriction is mediated by 20-hydroxyeicosatetraenoic acid (20-HETE) (a metabolite of arachidonic acid (AA) produced by cytochrome P450 4A enzymes (CYP450 4A) acting via thromboxane A_2/prostaglandin H_2 (TP) receptors and requires COX activity. CYP450 4A also produces reactive oxygen species (ROS), which contribute to the constriction. Whereas, in the brain stem supplied by the vertebro-basilar system larger arteries, such as basilar artery, dilate to flow. Dilation is mediated by NADPH-oxidase (activated by phosphatydilinositol3-kinase (PI3-K) derived H_2O_2 and/or eNOS derived nitric oxide (NO). eNOS is activated in an Akt-dependent pathway.*

All in all, regulation of cerebral blood flow (CBF) is the result of multilevel, interacting complex mechanisms aiming to maintain an appropriate blood flow thereby providing nutritional and gas supply for the brain tissue. To simplify, the tone of cerebral vessels is affected by both intraluminal pressure-induced constriction and flow-induced

dilation or constriction, “setting a basal vasomotor tone”, which is then modulated by metabolic, astrocytic-glial, neural signals providing the complex multilevel regulation of CBF. The sum of these mechanisms is capable to match the requirement of maintaining an appropriate blood flow for the brain tissue and in the same time complying with the limited space in the closed cranium.

I.6. SUMMARY OF NOVEL FINDINGS OF PART I.

1) Increases in flow elicit constrictions in isolated human intracerebral arteries and in rat middle cerebral arteries;
2) simultaneous increases of pressure and flow elicit significantly greater constriction than pressure alone in isolated rat middle cerebral arteries;
3) pressure- and flow-induced constriction together can achieve a more efficient estimated autoregulation of CBF than pressure alone;
4) the underlying subcellular mechanism of flow-induced constriction of cerebral arteries involves increased production of ROS, increased activity of COX and CYP450 enzymes and consequently increased production of 20-HETE, which acts via TP receptors.

Part II.

Dysfunctional pressure- and flow-induced vasomotor mechanisms in hypertension and aging. Pathophysiological effects on the autoregulation of CBF.

II.1. INTRODUCTION

The population in the Western world is aging and as hypertension affects most elderly people, these individuals are more likely to develop cerebrovascular pathologies.[141] For example, there is increasing evidence that in the elderly hypertension-induced microvascular injury promotes the development of vascular cognitive impairment (VCI)[142, 143] (which is the second most common cause of cognitive impairment after Alzheimer's disease) and increases the risk for hemorrhagic stroke.

Epidemiological studies provide strong evidence that the deleterious cerebrovascular effects of hypertension are also exacerbated in elderly patients, whereas young individuals appear to be more protected from cerebromicrovascular damage induced by hypertension.[144-146] Although the available human data suggest that advanced age and hypertension have synergistic effects, there are virtually no studies addressing the specific age-related mechanisms through which aging increases the vulnerability of the cerebromicrovascular system to hypertension leading to cerebrovascular diseases.[147]

Studies on young animals demonstrate that cerebral resistance arteries exhibit functional and structural adaptation to hypertension leading to increased vascular resistance, which provides and important protection of the distal portion of the cerebral microcirculation from pressure overload[63, 148]. Among these adaptive responses an increased pressure-induced myogenic constriction of cerebral resistance arteries is of great significance.[18, 22, 149] Previous studies demonstrated that in young hypertensive animals increased pressure sensitivity of the myogenic mechanism leads to an increased resistance at the level of the small cerebral arteries, keeping pressure in the thin-walled, injury-prone arterioles and capillaries in the normal range with little change in tissue blood supply and oxygenation. As a result of this adaptive response, the range of cerebral blood flow autoregulation is extended to higher pressure values both in hypertensive experimental animals and hypertensive patients.[63, 148, 150] Studies in animal models of hypertension and stroke[151] suggest that *pathological loss of autoregulatory protection contribute to cerebromicrovascular injury.* Despite the paramount

importance of the autoregulatory mechanisms in cerebromicrovascular protection, it is not well understood how aging affects the functional adaptation of the cerebral resistance arteries to maintain autoregulation of CBF in hypertension.

II.2. HYPOTHESIS AND AIMS OF STUDIES

The 2nd part of my work was designed to test the **hypothesis** that

1) aging and hypertension impairs functional adaptation of pressure- and flow-induced responses of cerebral vessels,

2) these are leading to impaired autoregulation of CBF, and

3) exacerbates hypertension-induced microvascular damage and neuroinflammation

4) promoting neural/learning dysfunction.

I **aimed** to asses in young and aged hypertensive mice:

1) the changes of arterial myogenic and flow-induced constriction and
2) autoregulation of cerebral blood flow
3) blood-brain barrier function, microvascular density
4) and markers of neuroinflammation and cognitive function.

II.3. MATERIAL AND METHODS

Animals

Young (3 month, n=80) and aged (24 month, n=80) male C57/BL6 mice and (to visualize pericytes) a cohort of young (3 month old) and aged (24 month old) α-SMA-GFP transgenic mice were used.[152] All mice were maintained under specific pathogen-free barrier conditions. Water and normal laboratory diet were available ad libitum. All procedures were approved by the Institutional Animal Use and Care Committees of the participating institutions.

Infusion of angiotensin II

To induce hypertension Alzet mini-osmotic pumps (Model 2006, 0.15 µl/h, 42 days; Durect Co, Cupertino, CA) were implanted into young and aged mice. Pumps were filled either with saline vehicle or solutions of Ang II (Sigma Chemical Co., St. Louis, Missouri,

USA) that delivered (subcutaneously) 1000 ng/min/kg of Ang II for 28 days.[153] Pumps were placed into the subcutaneous space of ketamine/xylazine anesthetized mice through a small incision in the back of the neck that was closed with surgical sutures. All incision sites healed rapidly without the need for any medication.

Blood pressure measurements

Systolic blood pressure of mice in each experimental group was measured by the tail cuff method (CODA Non-Invasive Blood Pressure System, Kent Scientific Co., Torrington, CT) before and 2 and 4 weeks after the minipump implantation.

Behavioral studies

Mice were assessed for learning capacity using an elevated plus maze-based learning protocol according to the methods of Carrie et al.[154] In brief, a gray elevated pus maze apparatus was used. Two open arms (25x5 cm) and two (25x5 cm) closed arms were attached at right angles to a central platform (5x5 cm). The apparatus was 40 cm above the floor. Mice were placed individually at the end of an open arm with their back to the central platform. The time for mice to cross a line halfway along one of the closed arms was measured (transfer latency) on day 1 and day 2. Mice had to have their body and each paw on the other side of the line. If a mouse had not crossed the line after 120 s, it was placed beyond it. After crossing the line, mice had 30 s for exploring the apparatus. Learning was defined as reduced transfer latency on day 2 compared to day 1st. For quantitative analysis a learning index was calculated based on relative difference in transfer latency on day 1 and day 2. Higher learning index indicates superior hippocampal function.

Cerebrovascular autoregulation

Animals were anesthetized with α-chloralose (50 mg/kg, i.p.) and urethane (750 mg/kg, i.p.), endotracheally intubated and ventilated (MousVent G500; Kent Scientific Co, Torrington, CT). Rectal temperature was maintained at 37^{o}C using a thermostatic heating pad (Kent Scientific Co, Torrington, CT). End-tidal CO_2 was maintained between 3.2% and 3.7%. The right femoral artery was cannulated for arterial blood pressure measurement (Living Systems Instrumentations, Burlington, VE). Mice were immobilized, placed on a stereotaxic frame, and the scalp and periosteum were pulled aside. Cortical blood flow was measured by laser speckle flowmetry (PeriCam PSI System, Perimed, Stockholm, Sweden) in a region of

interest placed between the bregma and lambda. After stabilization of MAP and blood gases, MAP was elevated or decreased in 20-mmHg steps by intravenous infusion of phenylephrine (1–2 μg/kg/min) or via controlled exsanguination (100–400 μl of arterial blood), respectively according to the protocols of Niwa et al.[155] The range of MAP studied was 40–160 mmHg. CBF values were recorded 5 min after MAP was changed. Changes in CBF were expressed relative to CBF corresponding to a systolic pressure of 80 mmHg[45]. Lower and upper limits of autoregulation were tested in separate animals because of potential pathological effects of changes in MAP above or below the autoregulation range.

Assessment of pressure- and flow-induced responses in isolated middle cerebral arteries

Mice were decapitated, the brains were removed and segments of the middle cerebral arteries (MCA) were isolated and studied in a pressure-flow myograph system as described in Part I. To test the autoregulatory function of MCAs both the static and dynamic components in the vascular myogenic response were assessed. The static component in the vascular myogenic response was assessed by measuring changes in vascular diameter in response to stepwise increases (10 mmHg steps, for 5 min each) in intraluminal pressure (from 0 to 180 mmHg). The dynamic component in the vascular myogenic response was assessed by measuring the time course of changes in vascular diameter in response to a sudden increase (from 60 to 160 mmHg) in intraluminal pressure.

To assess the role of 20-HETE in age- and hypertension-induced changes in the myogenic response, MCAs were incubated with HET0016 (10^{-6} mol/L, for 30 min, purchased from Cayman Chemical Company, Ann Arbor, MI). Then, vascular responses to stepwise increases in intraluminal pressure were reassessed. HET0016 was previously reported to selectively inhibit the formation of 20-HETE by inhibiting CYP4A and CYP4F isoforms in renal microsomes isolated from spontaneously hypertensive rats (IC_{50}: 35.2 nM) and in human kidney (IC_{50} : 8.9 nM). [156]

Previous studies showed that activation of transient receptor potential canonical type (TRPC6) channels mediate, at least in part, 20-HETE-induced vasomotor responses[157] and are involved in regulation of the myogenic response[158]. To assess the role of TRPC channels in age- and hypertension-induced changes in the myogenic response, MCAs were incubated with SKF96365 ($5x10^{-6}$ mol/L, for 15 min), a potent and specific blocker of transient receptor potential canonical type (TRPC) channels. Then, vascular responses to stepwise increases in intraluminal pressure were reassessed.

To assess flow-induced constriction in isolated MCAs intraluminal flow was increased in a stepwise manner by creating a pressure gradient through the vessel (from ΔP = 0 to 40 mmHg, corresponding to Q = 0 to 320 μL/min intraluminal flow) keeping intraluminal pressure constant. Intraluminal flow was measured with a micro-flow meter as reported.[159]

At the end of each experiment the passive diameter curves were obtained (0-180 mmHg) in the presence of Ca^{2+}-free Krebs' buffer containing nifedipine (10^{-5} mol/L) to achieve maximal vascular diameter.

Western blotting

Immunoblotting studies for TRPC6 in MCA homogenates and for the tight junction proteins (ZO-1, occludin, and claudin-5) in hippocampal homogenates were performed. In brief, MCAs and hippocampal samples from each animal (n=6 per experimental group) were homogenized in lysis buffer containing protease inhibitors. Samples were then subjected to SDS-Page gel electrophoresis and transferred to a PVDF membrane. Membranes were blocked with 5% BSA (in 2% Tween in PBS, for 2 h, at room temperature), incubated with primary antibody directed against TRPC6 (mouse monoclonal, 1:1000, overnight at 4 ^{o}C, Abcam), ZO-1 (clone R40.76 rat monoclonal, 1:500, overnight at 4 ^{o}C, Millipore), occludin (rabbit polyclonal, 1:1000; overnight at 4 ^{o}C, Abcam) or claudin-5 (rabbit polyclonal, 1:1000, overnight at 4 ^{o}C, Abcam), and then incubated with the appropriate HRP-conjugated secondary antibodies (for 2 h, at room temperature). Membranes were developed using Amersham ECL Prime Western Blotting Detection Reagent (GE Healthcare). The relative abundance of studied proteins was determined with densitometry and β-actin (mouse monoclonal, 1:15000, for 45 min, at room temperature, Abcam) as a loading control.

Quantitative real-time RT-PCR

A quantitative real time RT-PCR technique was used to analyze mRNA expression of the following genes in MCAs of mice from each experimental group: *Cyp4a12, Cyp4a10, Cyp4a14, Trpc6* using a Strategen MX3000 platform, as previously reported.[160] In brief, total RNA was isolated with a Mini RNA Isolation Kit (Zymo Research, Orange, CA) and was reverse transcribed using Superscript III RT (Invitrogen) as described previously.[160] Amplification efficiencies were determined using a dilution series of a standard vascular sample. Quantification was performed using the efficiency-corrected $\Delta\Delta$Cq method. The

relative quantities of the reference genes *Hprt, Ywhaz, B2m* and *Actb* were determined and a normalization factor was calculated based on the geometric mean for internal normalization. Fidelity of the PCR reaction was determined by melting temperature analysis and visualization of the product on a 2% agarose gel.

Assessment of the integrity of the blood brain barrier

A) Sodium fluorescein tracer assay. To assess the functional integrity of blood brain barrier (BBB) permeability we used the sodium fluorescein tracer assay according to the protocols of Kaya et al.[161]. In brief, mice were anesthetized by ketamin/xylazine (100/15 mg/kg, i.m.), and the a small water-soluble tracer sodium fluorescein (5 ml/kg, 2% in physiological saline, Sigma Aldrich, St Louis, MO) was administered intravenously by retroorbital injection. After 30 minutes of circulation of the tracer, animals were transcardially perfused with 1x heparin containing PBS. Then, the mice were decapitated and the brains were removed. From each brain the hippocampus, white matter and the prefrontal cortex were isolated and weighed. Samples were homogenized in 500µl ice-cold PBS and 500 µl 60% trichloroacetic acid was added to precipitate proteins. After 30 min incubation (at 4 ^{o}C) samples were centrifuged at 18,000 g (at 4°C, for 10 min). From the supernatants extravasated sodium fluorescein was quantified spectrophotofluorometrically (at an excitation wavelength of 440 nm and emission wavelength of 525 nm) using a microplate reader (Tecan Group Ltd, Mannedorf, Switzerland) and normalized to tissue weight. [162]

B) Demonstration of IgG extravasation by immunofluorescence. As an additional marker for increased hippocampal cerebrovascular permeability, IgG extravasation through the BBB was also demonstrated by immunofluorescent labeling and confocal microscopy (see below).

Immunofluorescent labeling and confocal microscopy

Anesthetized mice were transcardially perfused with PBS, then brains were removed and hemisected. The left hemispheres were fixed overnight in 4% paraformaldehyde, then they were cryoprotected in a series of graded sucrose solutions (10%, 20%, and 30% overnight), and frozen in Cryo-Gel (Electron Microscopy Sciences, Hatfield, PA). Coronal sections of 70 µm were cut through the hippocampus and stored free-floating in cryopreservative solution (25% glycerol, 25% ethylene glycol, 25% 0.2M phosphate buffer, 25% distilled water) at −20°C. Selected sections were ~1.6 mm caudal to Bregma,

representing the more rostral hippocampus. After washing (3x5 min with TBS plus 3x5 min with 1x TBS+0.25% TritonX-100), sections were treated with 1% of sodium-borohydride solution for 5 min. After a second washing step (3x5 min with distilled water plus 3x5 min with 1x TBS) and blocking in 5% BSA/TBS (with 0.5% Triton X-100, 0.3 M glycin and 1% fish gelatin; for 3 h), sections were immunostained using primary antibodies for 2 nights at 4°C. The following primary antibodies were used: mouse anti-CD31 (1: 100, phycoerythrin (PE) conjugated; Cat N: 553373, BD Pharmingen, San Jose CA; to label endothelial cells) or mouse anti-CD31 (1: 50, unconjugated; Cat N: 550274, BD Pharmingen, San Jose CA) to lable endothelial cells, mouse anti-IgG (1:100, FITC conjugated; Cat N: 005-090-003, Jackson Immuno Research, West Grove, PA) to label extravasated IgG, mouse anti-Iba1 (1:50, unconjugated; Cat N: 019-19741, Wako, Richmond, VA) to label microglia and mouse anti-CD68 (1:100, unconjugated; Cat N: ab125212, Abcam, Cambridge, MA) to label activated microglia. The following secondary antibodies were used: goat anti-rabbit IgG, Alexa Fluor 647 (1:1000, Cat N: 4414, Cell Signaling, Danvers, MA) and goat anti-rat IgG, Alexa Fluor 568 (1:1000, Cat N: A11077, Molecular Probes, Grand Island, NY). Sections were washed for 3x5 min with TBS plus 3x5 min with 1x TBS+0.25% TritonX-100. For nuclear counterstaining Hoechst 33342 was used. Then, the sections were transferred to slides and coverslipped. Confocal images were captured using a Leica SP2 MP confocal laser scanning microscope.

Pericyte coverage

Pericytes have key roles in maintenance of the BBB and preservation of the structural integrity of the cerebral microcirculation.[163] To assess age- and hypertension-induced changes in pericyte coverage of microvessels, in brain sections from young and aged αSMA-GFP transgenic mice with or without angiotensin II-induced hypertension immunolabeling for the endothelial marker CD31 was performed. For pericyte coverage, αSMA-GFP (which is abundantly expressed in pericytes) and anti-CD31 signals from microvessels $\leq$ 10 µm in diameter were separately subjected to threshold processing. The number of pericytes (identified as αSMA-GFP-positive cells with a typical pericyte morphology, long processes that extend over the capillaries, and perivascular localization with a Hoechst 33342-stained prominent round nucleus) per CD 31-positive capillary surface area per field was calculated. To confirm that αSMA-GFP positive cells on capillaries were indeed pericytes, we processed tissue sections for immunohistochemical staining using 1:200 rabbit polyclonal to

neuron/glia-type 2 antigen (NG2; Chemicon/Millipore, Billerica, MA) and 1:200 rat anti-mouse platelet-derived growth factor receptor (PDGFR)-β (eBioscience, San Diego, CA) antibodies. Sections were incubated in primary antibody for 42 h, washed 6 × 15 min in 1× TBS (1% Triton X-100), incubated for 3 h in 1:200 donkey anti-rabbit DyLight 549 (Jackson ImmunoResearch Laboratories, West Grove, PA) or goat anti-rat TRITC (Abcam). In addition, the areas occupied by the respective signals were analyzed using the area measurement tool of the MetaMorph software (version 7.7.9.0). Pericyte coverage was determined as a percentage (%) of α-SMA-GFP -positive pericyte surface area covering CD31-positive capillary surface area per filed. In each animal 4 randomly selected fields from the hippocampus were analyzed in 6 nonadjacent sections. Six animals per group were analyzed.

Capillary Density Analysis

Immunofluorescent labeling for CD31 (see above) was used to identify microvessels in the brain as we previously described.[164] Capillary density in the CA1, CA3, and dentate gyrus (DG) of the hippocampus, retrosplenial cortex (RSA), primary somatosensory cortex (S1) and corpus callosum (cc) was quantified as the length of blood vessels <10 μm in diameter per volume of tissue using Neurolucida with AutoNeuron (MicroBrightField, Williston, VT). Brain regions were identified based on reference[165]. The total length of capillaries (mm) was divided by the volume of brain tissue scanned (mm^3) to obtain capillary density (length per tissue volume).The density of CD31-stained capillaries was calculated within each region for each animal. The experimenter was blinded to the groups and treatments of the animals throughout the period of blood vessel staining and analysis.

Microglia activation

Immunofluorescent labeling for Iba1 and CD68 (see above) was used to identify microglia and activated microglia in the brain, respectively. The total number of Iba1 positive microglia and the number of CD68 positive activated microglia per region of interest in the hippocampus was calculated. In each animal 4 randomly selected fields from the hippocampus were analyzed in 6 nonadjacent sections. Six animals per group were analyzed.

Assessment of inflammatory gene expression in the hippocampus

In addition to quantifying microglia activation, we analyzed relative abundance of several neuroinflammatory cytokines/chemokines through quantitative real-time PCR with RNA isolated from snap-frozen hippocampal samples. Total RNA was isolated with RNeasy Mini kit (Qiagen) using a fully automated QIAcube-based workflow. Inflammatory gene expression was assessed using TaqMan® Gene Signature real-time PCR arrays (Mouse Immune Array and Alzheimer's Array; Applied Biosystems/Life Technologies, Carlsbad, CA).

Protein levels of microglia-derived inflammatory factors in the hippocampus

Previous studies reported that microglia activation is associated with a pro-inflammatory shift in the microglia secretome, including an increased production of including MCP-1, TNFα and IP-10. Thus, to further characterize neuroinflammation in our cohorts, protein levels of micoglia-derived pro-inflammatory factors (MCP-1, TNFα, IP-10) was analyzed in homogenates of the hippocampi using a magnetic bead array (Millipore, Billerica, MA). For normalization purposes the sample protein content was determined by a spectrophotometric quantitation method using BCA reagent (Pierce Chemical Co., Rockford, IL).

Determination of hippocampal protein 5-nitrotyrosine content

As a marker of hippocampal oxidative/nitrosative stress in hypertension and aging, 5-nitrotyrosine (5-NT; a marker for peroxynitrite action) was assessed in homogenates of hippocampi using the OxiSelect Protein Nitrotyrosine ELISA Kits (Cell Biolabs), according to the manufacturer's guidelines.

Statistical analysis

Data were analyzed by two-way analysis of variance (ANOVA) followed by Tukey post-hoc tests and Pearson's correlation analysis. A p value less than 0.05 was considered statistically significant. Data are expressed as mean±S.E.M.

II.4. RESULTS

Impaired cerebrovascular autoregulation in aged hypertensive mice

Blood pressure was significantly increased in both young and aged mice receiving Ang II infusion (Fig 11). In young control mice CBF was independent of blood pressure in the range of 60–120 mmHg, which indicates that autoregulation was present and effective (Fig.11). No differences in autoregulation were observed among young and aged normotensive mice (Fig. 11). In young hypertensive mice, however, the relationship between blood pressure and CBF was substantially altered. There was a progressive expansion of the range of autoregulation, indicating an adaptive response (Fig. 11), which was completely absent in aged hypertensive mice. In aged hypertensive mice, the relationship between blood pressure and CBF was essentially linear, which indicates total dependence of CBF on blood pressure and loss of autoregulation (Fig. 11).

Aging impairs autoregulatory function of cerebral arteries: role of myogenic and flow-induced constriction

Fig. 11 shows myogenic constriction developed in isolated MCAs at intraluminal pressures of 20–180 mmHg. In MCAs of young control mice, increases in intravascular pressure increased myogenic constriction up to 60 mmHg, and myogenic tone was maintained at almost the same level at up to ~120 mmHg, which overlaps the autoregulatory range of CBF. At higher pressures myogenic tone then tended to decrease and arteries tended to dilate gradually (Fig. 11). Myogenic constriction in MCAs from young hypertensive mice was significantly enhanced and the myogenic tone was maintained at almost the same level at up to ~160 mmHg, which corresponds to the increased autoregulatory range of CBF in these animals. MCAs of aged mice developed a slightly decreased myogenic constriction and did not exhibit a similar hypertension-induced adaptive increase in myogenic constriction, which was observed in young mice (Fig.11).

It is an important role of the myogenic mechanism to prevent sudden increases in perfusion pressure in the distal part of microcirculation by increasing arteriolar resistance when pressure increases. Thus, we investigated the time-dependent behavior of the myogenic response as well.

In MCAs of young control mice a step increase in intraluminal pressure from 60 to 140 mmHg resulted only in slight increase in diameter (Fig. 11). In MCAs of young hypertensive

mice the myogenic constriction was enhanced, no increase in diameter was observed. In contrast, MCAs of aged mice could not maintain resting tone and did not exhibit a hypertension-induced adaptive increase in myogenic constriction (Fig.11).

Increases in intraluminal flow elicited vasoconstriction in MCAs of young mice and this response was significantly enhanced by hypertension (Fig. 11). In contrast, there was no adaptive increase in flow-induced constriction in MCAs of aged hypertensive mice (Fig. 11).

Role of 20-HETE and TRPC6 in functional maladaptation of aged cerebral arteries to hypertension

To assess the role of 20-HETE in functional adaptation of cerebral arteries to hypertension, we tested the direct effect of extraluminal HET0016 on myogenic constriction of cerebral vessels at a pathophysiologically relevant pressure range (≥160 mmHg; Fig. 12). Because we found that in mouse arteries the vasoconstrictor effect of 20-HETE is significantly inhibited by the TRPC6 inhibitor SKF96365 (data not shown) we also assessed the role of TRPC6 channels in 20-HETE-dependent functional adaptation of cerebral arteries to hypertension using SKF96365. We found that in MCAs of young hypertensive mice increased myogenic tone was significantly inhibited by both HET0016 (Fig. 12) and SKF96365 (Fig. 13) eliminating the difference between the four groups, whereas neither HET0016 nor SKF96365 affect significantly the myogenic tone of MCAs of aged hypertensive mice. HET0016 (Fig. 12 and 13) and SKF96365 (not shown) also inhibited the enhanced dynamic component of myogenic constriction and flow-induced constriction in MCAs of young hypertensive mice, whereas it had no significant effects in MCAs of aged hypertensive mice.

Hypertension was associated with up-regulated expression of the CYP 4A arachidonic acid ω-hydroxylases *Cyp4a12*, *Cyp4a10* and *Cyp4a14* (Fig. 2F-H) and TRPC6 channels (Fig. 12 and 13) in MCAs of young mice, whereas these adaptive responses were significantly impaired or missing in MCAs of aged hypertensive mice.

Aging exacerbates hypertension-induced BBB disruption

Using a sodium fluorescein tracer assay we tested the hypothesis that cerebrovascular autoregulatory dysfunction in aged hypertensive mice leads to BBB disruption. As predicted by our model, we found that aging exacerbates hypertension-induced fluorescein leakage in the hippocampi, cortex and white matter (Fig. 14). Aging *per se* also tended to increase the

fluorescein leakage, but these changes reached statistical significance only in the cortex and white matter. We hypothesized that the aging hypertensive brain also cannot maintain the BBB in vivo against endogenous circulating macromolecules, some of which exert significant pro-inflammatory and, potentially, neurotoxic effects. Immunostaining for plasma-derived IgG revealed significant perivascular IgG deposits and >10-fold increase in IgG accumulation in the hippocampus of aged hypertensive mice (Fig. 14). IgG leakage in the hippocampus of young hypertensive mice was significantly reduced and there was no detectable IgG leakage in young control mice. BBB breakdown in neurodegenerative disorders often indicates disruption of the tight junctions due to reduced expression of tight junction proteins.[166] In that regard it is significant that in the hippocampi of aged hypertensive mice their expression also tends to be down-regulated (Fig.14), although these alterations *per se* are unlikely to explain exacerbation of hypertension-induced BBB disruption in aging.

Aging exacerbates hypertension-induced pericyte loss and microvascular rarefaction

Because recent studies demonstrate that pericyte loss can compromise BBB integrity,[167] we assessed age- and hypertension-induced changes in pericyte coverage of hippocampal microvessels (Fig. 15). In young mice hypertension resulted in a significant decline in the relative number of pericytes (Fig. 15) and capillary pericyte coverage (by ~29%). In aged mice hypertension-induced decreases in pericyte number (Fig. 15) and pericyte coverage (by ~41%) were exacerbated. We also determined whether pericyte loss influences brain capillary density in the aged hypertensive mice. Capillaries were identified by their expression of CD31, using a lumen diameter of 10 μm or less as a standard identifier. As shown in Fig. 15 relative hypertension-induced decreases in capillary length density in CA1, CA3, and DG of the mouse hippocampus, retrosplenial cortex, primary somatosensory cortex and corpus callosum of aged mice were significantly greater than in young mice.

Aging exacerbates hypertension-induced inflammation and oxidative stress in the hippocampus

Previous studies suggest that leakage of plasma-derived factors through the damaged BBB has the potential to induce neuroinflammation by activating microglia.[166] In the hippocampi of young mice the number of activated microglia was low and hypertension-induced changes in microglia activation did not reach statistical significance. We found that aging is associated with a relative increase in the number of activated microglia in the

hippocampi. Importantly, hypertension-induced microglia activation was exacerbated in the hippocampi of aged mice (Fig. 16). Sustained activation of microglia was associated with an increased expression of several pro-inflammatory cytokines and chemokines (Fig. 16) and other inflammatory mediators (data not shown) in the hippocampi of aged hypertensive mice. These findings were corroborated by demonstration of increased protein expression of MCP-1, TNFα and IP-10 (Fig. 16), which are known to be secreted by activated microglia, in the hippocampi of aged hypertensive mice.

Neuroinflammation is frequently associated with increased oxidative stress. Consistent with the presence of hypertension-related oxidative/nitrosative stress in the brain,[168] hippocampal 5-nitrotyrosine content was increased in young hypertensive mice (Fig. 16). Aging exacerbated hypertension-induced increases in hippocampal 5-nitrotyrosine content (Fig. 16), confirming that the effects of age and hypertension are synergistic.

Aging exacerbates hypertension-induced decline in hippocampal dependent learning

In young control mice, transfer latency on Day 2 was significantly decreased compared to Day 1 (Fig. 17), indicating an intact learning effect (learning index: 1). The learning indexes for young hypertensive mice (~0.7) and aged (~0.67) mice tended to decrease, compared to young control mice, although the differences did not reach statistical significance. For old hypertensive mice, transfer latency was similar on Days 1 and 2 (corresponding to a learning index: ~0). This can be interpreted that these mice had significantly impaired hippocampal dependent cognitive function.

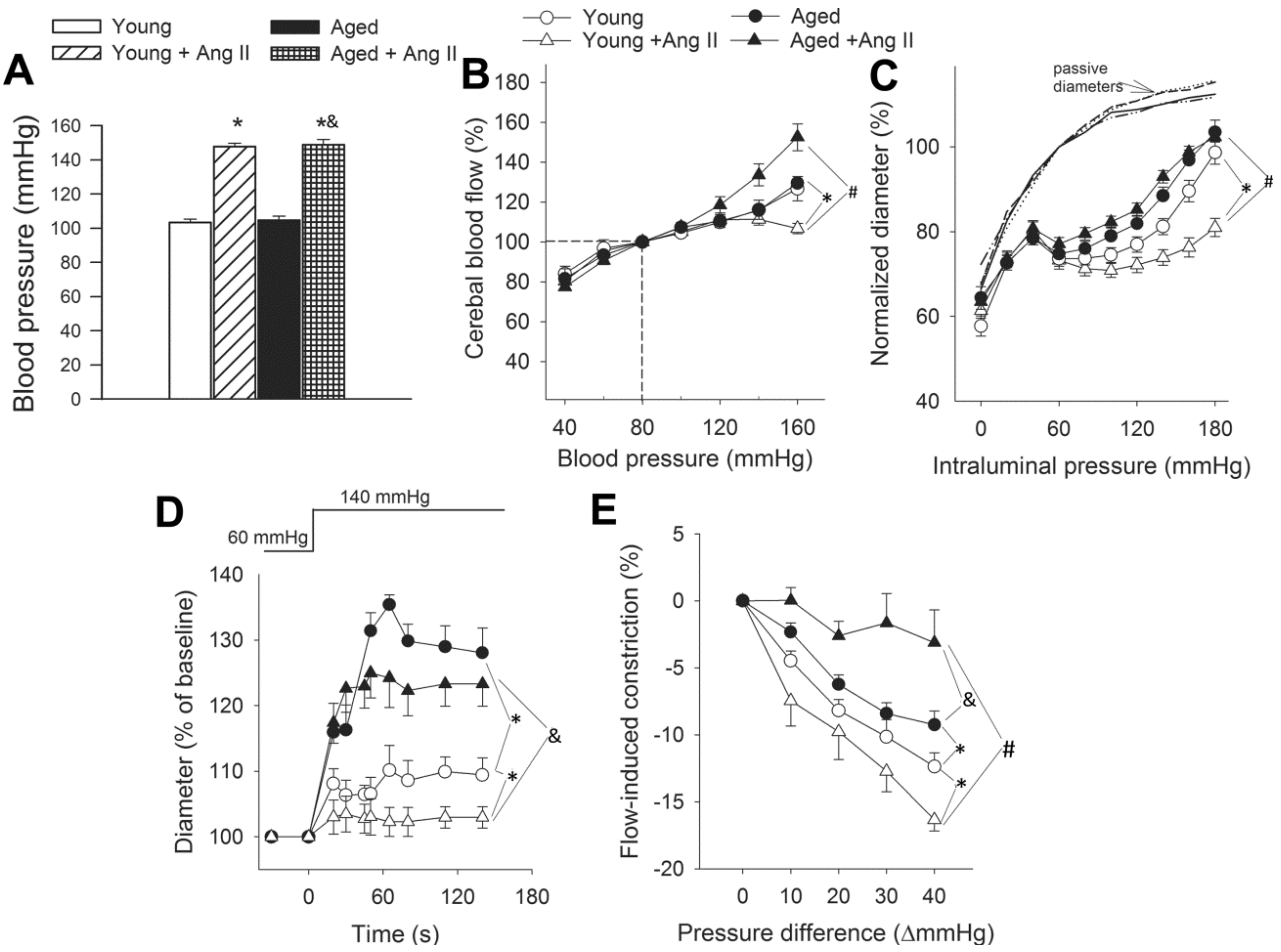

Figure 11. Aging impairs adaptation of cerebrovascular autoregulation to hypertension. ***Panel A:*** *Effect of chronic infusion of angiotensin II on systolic blood pressure in young and aged mice. Data are mean ± S.E.M. (n=20-25 for each group) *P<0.05 vs.Young; [&] P<0.05 vs. Aged.* ***B****: Relationship between CBF and systolic blood pressure in young control, young hypertensive (Young+AngII), aged control and aged hypertensive (Aged +AngII) mice. Data are mean±S.E.M.(n=8). In young control mice, CBF is statistically different from the value at 100 mmHg at pressure values of <60 and >140 mmHg, indicating the autoregulatory range. In young hypertensive mice, there was a progressive expansion of the range of autoregulation range, indicating an adaptive response (*P<0.05 vs.Young), which was completely absent in aged hypertensive mice([#]P<0.05 vs.Young +AngII).* ***C:*** *Steady-state changes in diameter of middle cerebral arteries (MCA) isolated from each experimental group of mice in response to increases in intraluminal pressure, representing the static component of the myogenic response. Vascular diameters are expressed as percentage of the maximally dilated passive diameter of each vessel at 80 mmHg.* ***D:*** *Changes in the diameter of MCAs to a sudden increase in intraluminal pressure (from 60 to 140 mmHg), representing the dynamic component of the myogenic response.* ***E:*** *Flow-induced constriction of MCAs (induced by increasing intraluminal flow by creating a pressure gradient through the vessels). Data are mean±S.E.M.(n=8-16). *P<0.05 vs.Young; [#]P<0.05 vs.Young+AngII;. [&]P<0.05 vs.Aged.*

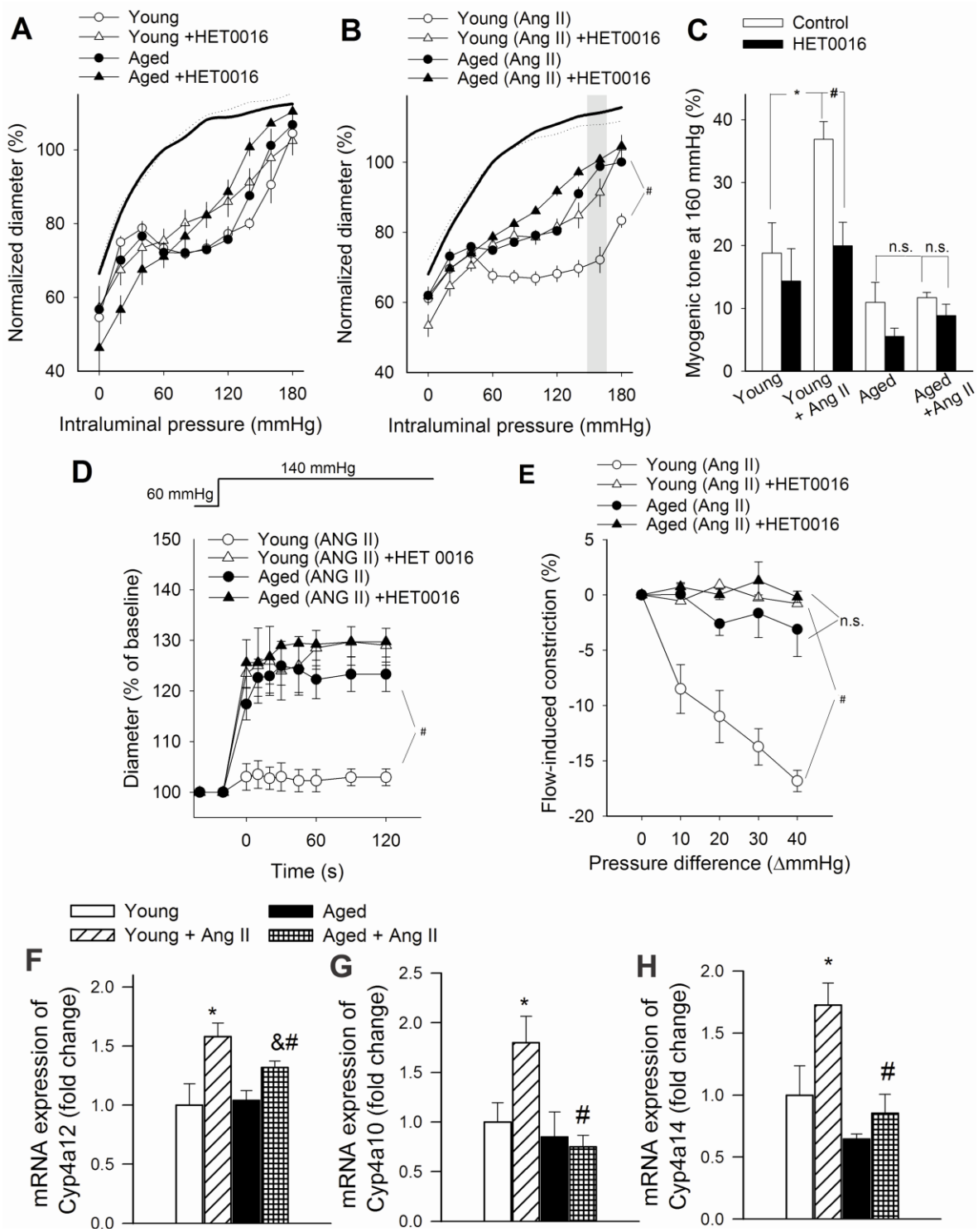

Figure 12. Role of 20-HETE mediation in cerebrovascular autoregulatory dysfunction in aged hypertensive mice. Panels A-B: *The effect of HET0016 (10^{-6} mol/L), an inhibitor of 20-HETE synthesis, on myogenic constriction of middle cerebral arteries(MCA) isolated from young control, young hypertensive (Young+AngII), aged control and aged hypertensive(Aged+Ang II) mice in response to increases in intraluminal pressure. Vascular diameters are expressed as percentage of the passive diameter of the vessels at 80 mmHg.* ***C****: Myogenic tone of MCAs in the absence and presence of HET0016 at an intraluminal pressure of 160 mmHg. Data are mean±S.E.M. (n=8 in each group). *P<0.05 vs.young; #P<0.05 vs. Young+AngII.* ***D-E:*** *Effect of HET0016 on the early rapid phase of the myogenic response (D; induced by a sudden increase in intraluminal pressure from 60 to 140 mmHg) and flow-induced constriction (E; induced by increasing intraluminal flow by creating a pressure gradient through the vessels; see Methods) of MCAs. Data are mean±S.E.M. (n=8-16). #P<0.05 vs. Young+Ang II.* ***F -H:*** *QRT-PCR data showing mRNA expression of cytochrome P450 4A enzymes in MCAs. Data are mean±S.E.M. (n=6 in each group). *P<0.05 vs. Young; #P<0.05 vs .Young+Ang II; & P<0.05 vs. Aged.*

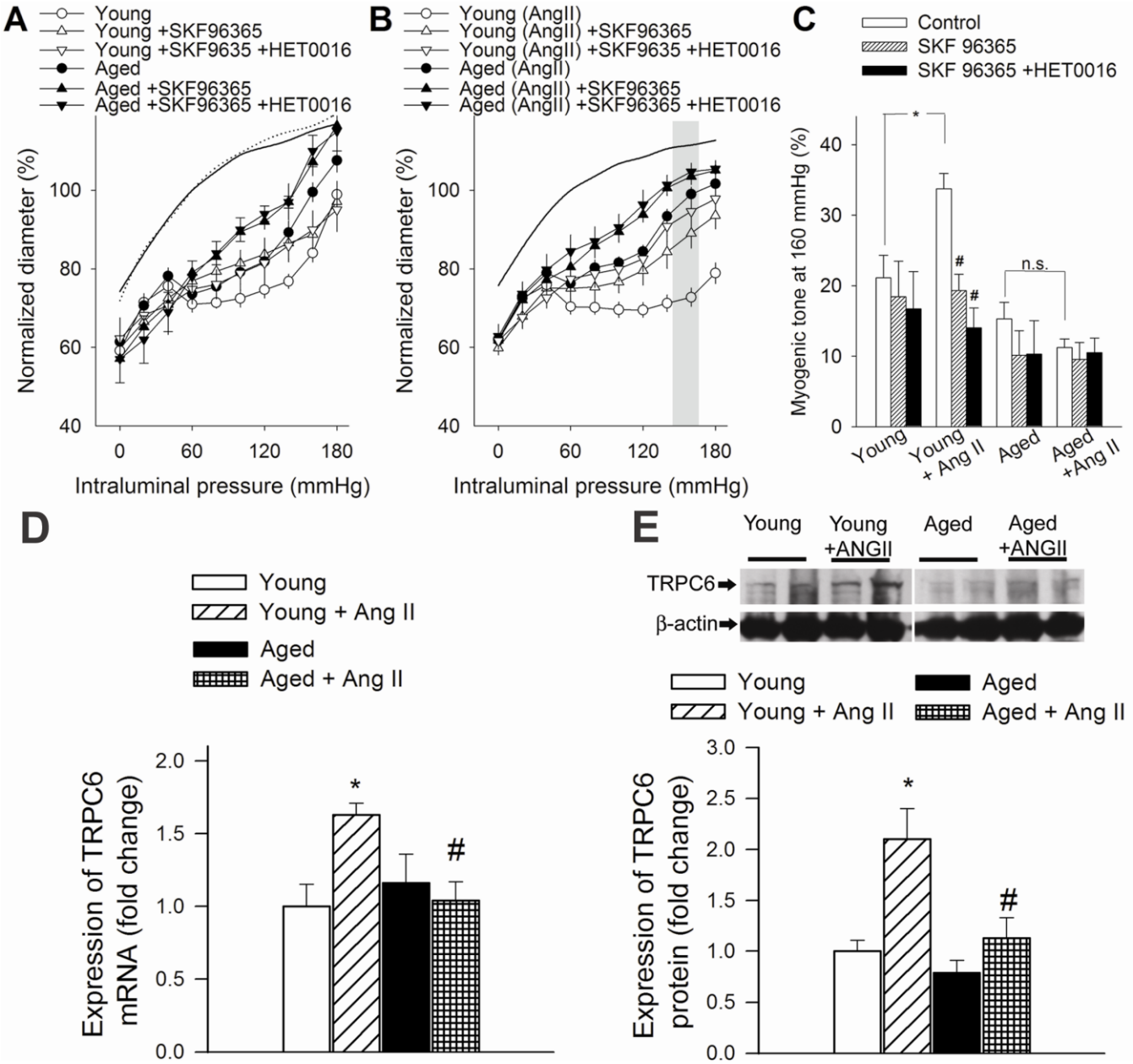

Figure 13. Role of TRPC6 in cerebrovascular autoregulatory dysfunction in aged hypertensive mice. Panels A-B: *The effect of SKF96365 (5 µmol/L), a TRPC channel blocker, and HET0016 (10^{-6} mol/L), an inhibitor of 20-HETE synthesis, on myogenic constriction of middle cerebral arteries(MCA) isolated from young control, young hypertensive (Young+Ang II), aged control and aged hypertensive (Aged+Ang II) mice. Vascular diameters are expressed as percentage of the passive diameter of the vessels at 80 mmHg.* ***C****: myogenic tone of MCAs in the absence and presence of SKF96365 and HET0016 at an intraluminal pressure of 160 mmHg. Data are mean±S.E.M. (n=8 in each group). *P<0.05 vs. Young; #P<0.05 vs.Young+Ang II.* ***D-E:*** *mRNA(D; QRT-PCR data) and protein expression E; Western blotting) of TRPC6 in MCAs. Data are mean±S.E.M. (n=6 in each group). *P<0.05 vs. Young; #P<0.05 vs. Young+Ang II.*

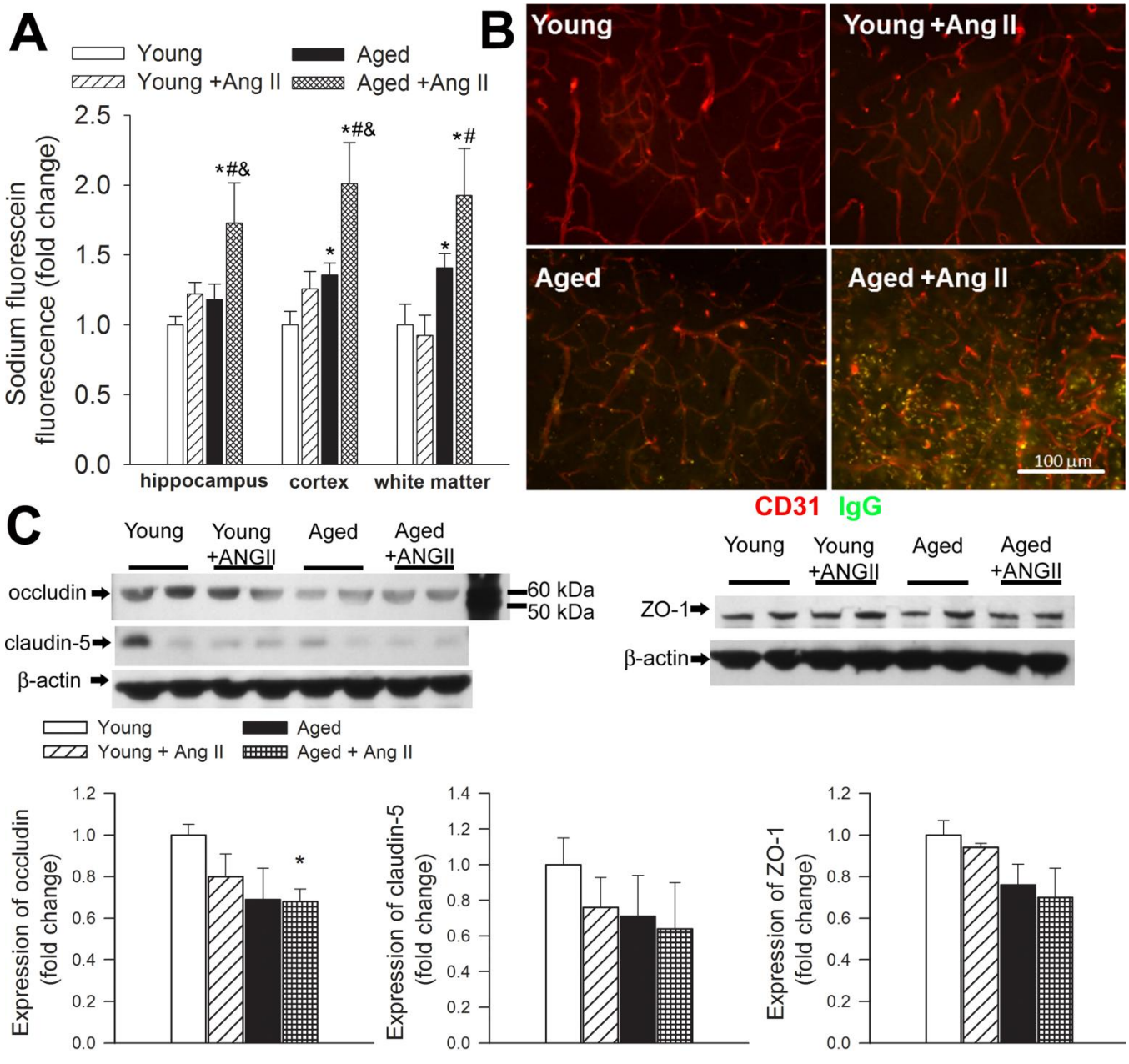

Figure 14. Aging exacerbates hypertension-induced disruption of the blood-brain barrier. A: *Hypertension and aging-induced changes in sodium fluorescein content in the hippocampus, cortex and white matter of young control, young hypertensive (Young+Ang II), aged control and aged hypertensive (Aged +Ang II) mice. Data are mean±S.E.M. *P<0.05 vs. Young, $^{\#}$P<0.05 vs. Young + Ang II; $^{\&}$P<0.05 vs. Aged (n=6 to 10).* ***B****: Confocal microscopy analysis of plasma-derived IgG (green) and CD31-positive microvessels(red) in the hippocampus of young and aged mice with or without Ang II-*induced *hypertension. Note the increased presence of extravascular IgG deposits in the hippocampus of aged hypertensive mice.* ***C:*** *Expression of occludin, claudin-5 and ZO-1 in the hippocampi of young and aged normotensive and hypertensive mice. Upper panels: original Western blots. β-actin was used as a loading control. Bar graphs are summary densitometric values. Data are mean ± S.E.M. *P<0.05 vs. Young. n=6 animals per group.*

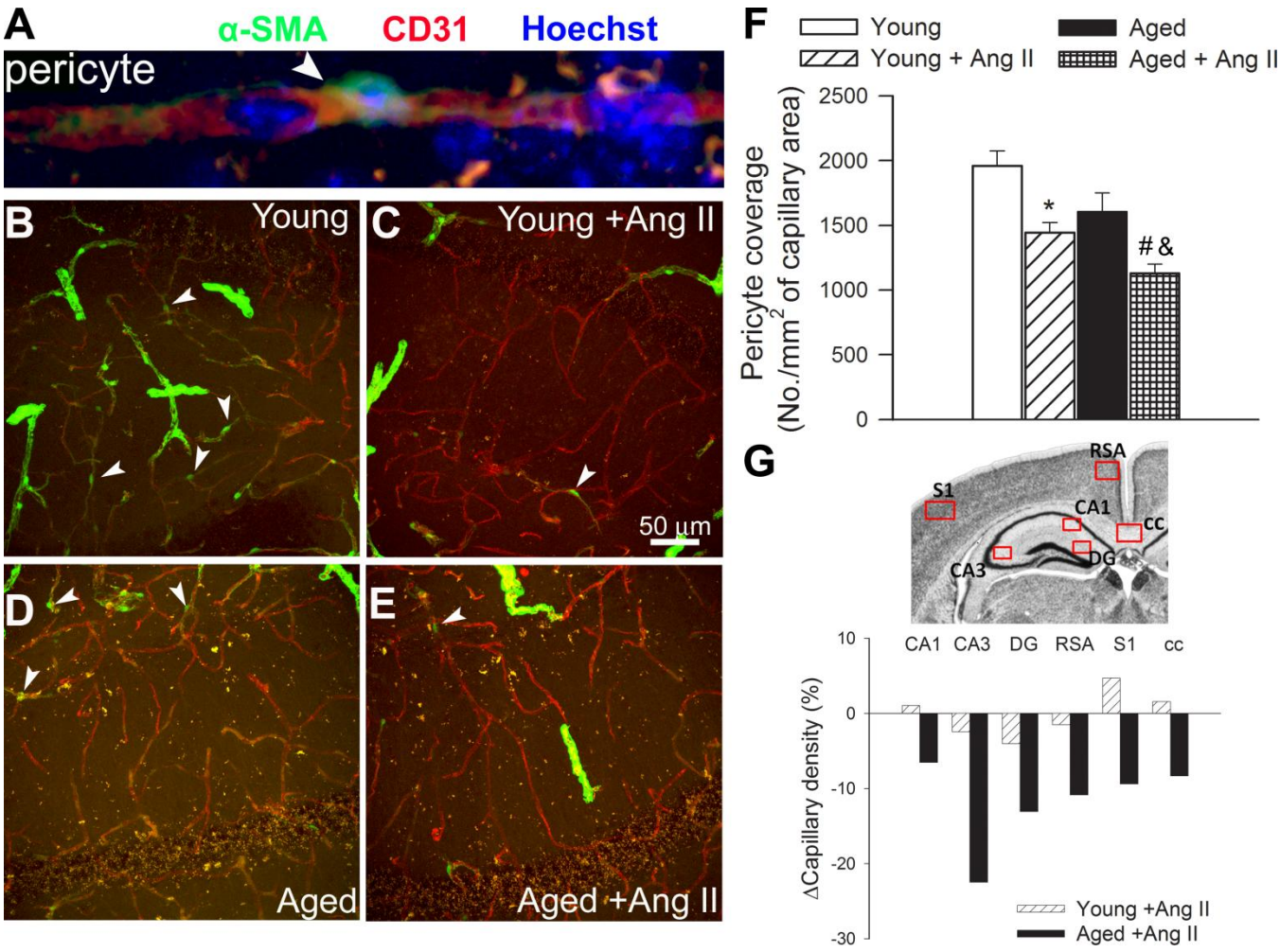

Figure 15. Hypertension-induced changes in pericyte coverage of hippocampal capillaries and hippocampal capillary density. ***A****: Representative confocal image showing perivascular localization of an α-smooth muscle actin (αSMA) expressing pericyte (green, arrowhead) surrounding CD31-positive capillary endothelial cells (red) in the CA1 region of the mouse hippocampus. Hoechst 33342 was used for nuclear counterstaining. B-E: Representative confocal microscopy analysis of α-SMA expressing pericyte coverage(green, arrowheads) of CD31-positive capillaries(red) in the CA1 region of the hippocampi of young control (****B****), young hypertensive (Young+Ang II)(****C****), aged control(****D****) and aged hypertensive (Aged +Ang II) (****E****) animals. Note that αSMA expressing pericytes (arrowheads) and vascular smooth muscle cells surrounding the terminal arterioles exhibit different morphologies.* ***F****: Summary data showing hypertension-dependent loss of pericyte coverage in the hippocampus (see Supplemental Experimental Procedures for details). *P<0.05 vs. Young; $^{\#}$P<0.05 vs. Young + Ang II; $^{\&}$P<0.05 vs. Aged.* ***G****: Hypertension-induced relative changes of capillary density in the CA1 and CA3 regions of the hippocampus, dentate gyrus (DG), retrosplenial cortex(RSA), primary somatosensory cortex(S1) and corpus callosum(cc) of young and aged mice. Boxes indicate brain regions that were included in the evaluation of capillary density (see the extended Methods section for details).*

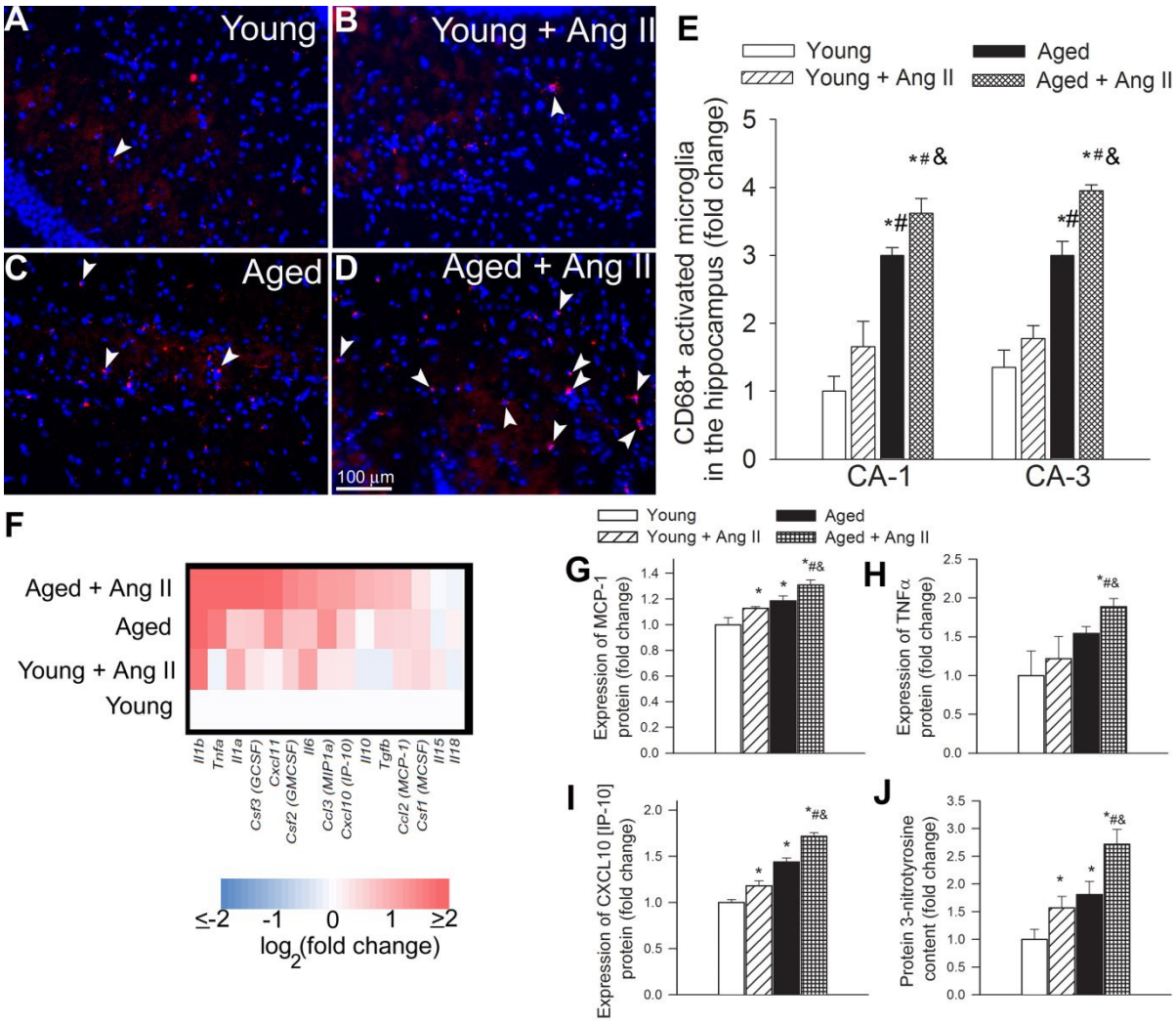

Figure 16. Aging exacerbates hypertension-induced neuroinflammation and cognitive decline. ***Panels A-D****: CD68 positive(red fluorescence, arrowheads) activated microglia in the hippocampus CA-1 region from young control(A), young hypertensive (Young+Ang II) (B), aged control (C) and aged hypertensive(Aged +AngII) (D) animals(blue fluorescence: nuclei).* ***Panel E*** *depicts summary data of relative changes in the number of CD68 positive activated microglia in the CA-1 and CA-3 regions of hippocampus (fold change). Data are mean±S.E.M. *P<0.05 vs. Young; #P<0.05 vs. Young + Ang; & P<0.05 vs. Aged.* ***F****: Hypertension in aging is associated with a pro-inflammatory shift in cytokine expression profiles in the mouse hippocampus. The heat map is a graphic representation of normalized mRNA expression of cytokines and chemokines depicted by color intensity, from highest (bright red) to lowest(bright blue) expression(n=6 in each group). Aged hypertensive mice have the highest expression of inflammatory markers.* ***G-I:*** *Relative hippocampal levels of micoglia-derived pro-inflammatory cytokines MCP-1(G), TNFα (H) and IP-10 (I) and 5-nitrotyrosine (a marker for peroxynitrite action; J). Data are mean±S.E.M. *P<0.05 vs. Young; #P<0.05 vs. Young + Ang II; &P<0.05 vs. Aged.*

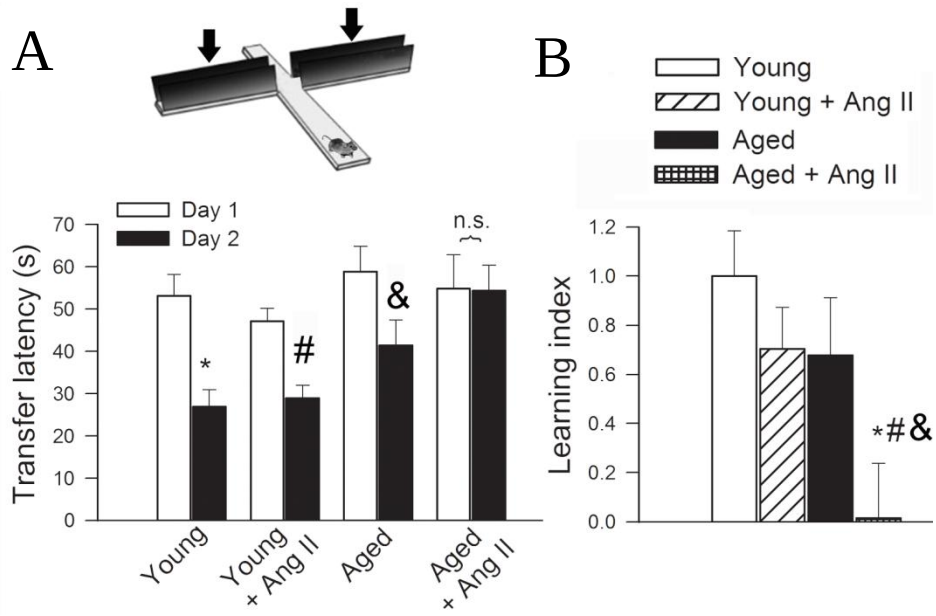

Figure 17. Aging exacerbates hypertension-induced cognitive impairment*. **A:** For old hypertensive mice, transfer latency was similar on Days 1 and 2 (corresponding to a learning index: ~0 **B**), indicating that these mice had significantly impaired hippocampal cognitive function. Data are mean±S.E.M. *P<0.05 vs. Young; #P<0.05 vs. Young + Ang II; &P<0.05 vs. Aged.*

II.5. DISCUSSION OF FINDINGS

In the cerebral circulation myogenic constriction of proximal branches of the cerebrovascular tree (i.e. MCA) is uniquely important for protection of the distal cerebral microcirculation.[34] In healthy young animals pressure-induced myogenic constriction of the cerebral arteries (Fig. 11) acts as a critical homeostatic mechanism that assures that increased arterial pressure does not penetrate the distal portion of the microcirculation, causing damage to the thin-walled arteriolar and capillary microvessels in the brain.[18, 149] In hypertensive young mice (Fig. 11) and rats[22, 169] the myogenic constriction of cerebral arteries is enhanced and the range of cerebrovascular autoregulation is extended, which represent functional adaptation of these vessels to higher systemic blood pressure, protecting the cerebral microcirculation.[18, 22, 63, 148, 149] We have found perhaps for the first time that cerebral arteries of aged mice do not exhibit a hypertension-induced adaptive increase in myogenic constriction observed in young mice (Fig. 11).

As we have shown (Part I of the thesis) in addition to the myogenic response flow-induced constriction of cerebral arteries may also contribute to cerebrovascular autoregulatory function.[23, 170] We have demonstrated that in young hypertensive mice flow-induced arterial constriction is also enhanced (Fig. 11), representing another component of functional arterial adaptation to high blood pressure. This adaptive response is also impaired in aged hypertensive mice (Fig. 11). Taken together, hypertension in aging is associated with dysfunction of cerebrovascular autoregulatory mechanisms protecting the brain. Interestingly, aging *per se* is associated with an impairment of both flow-induced constriction and the dynamic component of the myogenic response (Fig. 11), suggesting that during sudden increases in intraluminal pressure (for example during Valsalva-maneuver and similar conditions) in aged normotensive animals higher blood pressure may temporarily penetrate the distal portion of the cerebral microcirculation, which could lead to hemorrhagic stroke.

Several lines of evidence support the view that in young animals activation of a 20-HETE/TRPC6-dependent pathway underlies functional adaptation of cerebral arteries to hypertension and that this adaptive response is dysfunctional in aging. First, in young hypertensive mice 20-HETE mediation of myogenic constriction is up-regulated in the physiologically relevant high pressure range, likely due to adaptive up-regulation of cytochrome P450 4A ω-hydroxylases (Fig. 12). Similarly, in young hypertensive rats pressure-induced 20-HETE production in cerebral arteries is also significantly increased.[128] We have found that this, 20-HETE-dependent adaptive response is impaired in aged hypertensive mice (Fig. 12). Previous studies demonstrate that activation of TRPC6 channels mediates 20-HETE-induced increases in intracellular Ca^{2+} levels in vascular smooth muscle cells[171] and contributes to myogenic constriction of cerebral arteries[172] and while in cerebral arteries of young mice hypertension up-regulates vascular TRPC6 expression and activity (Fig. 13), this adaptive response is impaired in aged hypertensive mice. Because flow-induced constriction of cerebral arteries is predominantly mediated by 20-HETE,[23, 94] dysregulation of this pathway in aged hypertensive mice simultaneously impairs both the myogenic and the flow-induced components of cerebrovascular autoregulation. Because inhibition of the 20-HETE/TRPC6 pathway does not completely abolish myogenic constriction in cerebral arteries of young hypertensive mice, we cannot exclude a potential role for other mechanisms in functional maladaptation to hypertension in aging as well, including pathways involved in cellular calcium homeostasis in the vascular smooth muscle cells. The age-related mechanism(s) that are responsible for dysregulation of cytochrome

P450 4A ω-hydroxylases are presently unknown and may include an age-related IGF-1 deficiency.[173] In support of this concept, there are data extant showing that IGF-1 deficiency in mice is associated with impaired hypertension-induced adaptive changes in cerebral arterial myogenic tone (Toth and Ungvari, unpublished observation 2012) and down-regulation of *Cyp4a12b* expression (GEO datasets GDS2019 and GDS1053), mimicking the aging phenotype.

We found evidence that autoregulatory dysfunction in aged hypertensive mice leads to significant cerebromicrovascular damage. Lack of autoregulatory protection likely allows high blood pressure to penetrate the distal portion of the cerebral microcirculation, which leads to significant BBB disruption in the hippocampus and other brain regions in aged hypertensive mice (Fig. 14). The mechanisms of hypertension-induced BBB disruption are likely multifaceted and may involve increased oxidative stress[174]. Pericytes are important cellular constituents of the BBB and they are sensitive to oxidative stress. Thus, it is likely that increased hypertension-induced loss of pericyte coverage (Fig. 15) contributes to BBB disruption in aged mice. This view is supported by the findings that in *Pdgfrβ*$^{+/-}$ mice pericyte deficiency leads to significant impairment of BBB function[167] and development of a VCI-like syndrome. The mechanisms of increased pericyte loss in aged hypertensive mice are presently unknown. Pericytes are sensitive to oxidative damage, thus it is possible that exacerbated hypertension-induced oxidative stress contributes to the increased pericyte loss in aged mice. Pericytes have key roles in preservation of the structural integrity of the cerebral microcirculation,[163] thus, loss of pericytes is also likely to contribute to microvascular rarefaction in brain of aged hypertensive mice. Future studies should elucidate whether decreased capillary density in aged hypertensive mice is associated with reduced hippocampal blood flow leading to ischemic foci, which would have a direct deleterious effect on learning/cognitive function. In that regard it is significant that angiotensin II-induced hypertension also impairs endothelial regulation of and cerebral microcirculation by increasing oxidative/nitrosative stress in endothelial cells.[175, 176] Microvascular endothelial dysfunction likely also negatively impact cerebral blood supply and thereby may exacerbate neuronal dysfunction in aged hypertensive mice.

Increased BBB disruption in aged hypertensive mice is likely to impair neuronal function by multiple mechanisms, including alterations in the ionic microenvironment around synapses. Another highly important mechanism is the induction of neuroinflammation. Through the damaged BBB plasma constituents, including IgG, enter the brain, which have

the potential to activate microglia via the IgG Fc receptors. Activation of the IgG Fc receptor in the brain by plasma-derived IgG was recently shown to confer deleterious neuronal effects.[177] We have found evidence that in aged hypertensive mice BBB disruption results in increased extravasation of IgG (Fig.14) and an exacerbated neuroinflammatory response as shown by the increased number of activated microglia in the hippocampi (Fig. 16). We also found that in the hippocampi of aged hypertensive mice there is an increased presence and expression of inflammatory mediators (Fig. 16), which are known to be secreted by activated microglia. Microglia-derived pro-inflammatory cytokines, chemokines and proteases (i.e. MMPs) are thought to play a role in neuronal dysfunction and neurodegeneration in various pathophysiological conditions,[178] suggesting that exacerbation of neuroinflammation may importantly contribute to hypertension-induced neuronal dysfunction in aged mice (Fig. 17). Further, it is possible that vascular-derived inflammatory mediators also contribute to neuroinflammation in hypertensive aged mice.[179] Activated microglia are also known to exhibit increased production of free radicals, thereby causing oxidative neuronal injury.[180] Previous studies suggest that enhanced microglia-derived ROS production, perhaps acting in synergy with increased ROS derived from microvascular sources,[175, 176] may contribute to neuroinflammation-induced hippocampal dysfunction. Our findings that aging exacerbates hypertension-induced oxidative/nitrosative stress in the hippocampus (Fig. 16) are consistent with this view.

To determine whether compromised BBB integrity, microvascular rarefaction, oxidative/nitrosative stress and chronic low-grade neuroinflammation were sufficient to induce neuronal dysfunction in aged hypertensive mice, we studied behavior. Importantly, hypertensive aged mice had the worst performance on behavioral tests of hippocampal function (Fig. 17).

The available human evidence[181] suggests that increased BBB permeability in the elderly also associates with cognitive impairment.

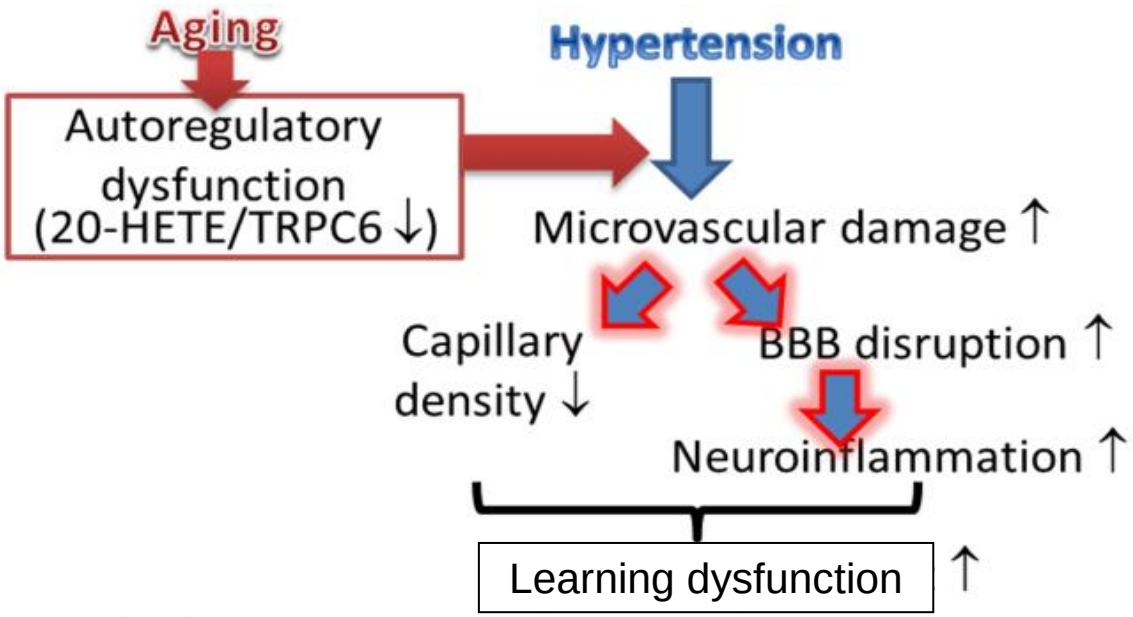

Figure 18. *Proposed scheme depicting the mechanisms by which age-related cerebrovascular autoregulatory dysfunction (due to lack of up-regulation of 20-HETE/TRPC6 pathway) exacerbates hypertension-induced microvascular damage, blood-brain barrier (BBB) disruption and neuroinflammation leading to learning/cognitive impairment.*

In conclusion, we found that aging in mice exacerbates hypertension-induced cerebromicrovascular injury and BBB disruption due to an age-related autoregulatory dysfunction, which induces neuroinflammation and promotes the development of learning/cognitive impairment. Our findings have important clinical relevance. There are randomized studies which evaluated learning decline as an outcome with treatment of hypertension in elderly patients. In the PROGRESS[182] and Syst-Eur[183] studies treatment of hypertension resulted in a 19% and 50% reduction in dementia incidence, respectively. Among elderly patients with hypertension with mild cognitive impairment the SCOPE study also found evidence suggesting that treatment with candesartan (an AT1 receptor antagonist) may prevent cognitive decline.[184] Thus it is likely that impairment of vasomotor responses to hemodynamic forces in aging and hypertension contribute to the development of these pathological conditions.

On the basis of our findings one can also hypothesize that treatment of hypertension in elderly patients with different pharmacological agents may have differential effect on learning and cognitive function, depending on the effect of the drugs on cerebral autoregulatory function. For example, a drug that impairs myogenic reactivity in cerebral

resistance arteries is actually expected to have a negative effect on learning/cognitive function. Further studies are warranted to test this hypothesis, which should also elucidate the specific age-related mechanism that underlies impaired adaptation of aged cerebral vessels to hypertension, including the role of age-related changes in endocrine factors.[173]

The clinical relevance of our findings is exampled when there is a sudden, larger increase in blood pressure, such as Valsalva maneuver and other similar conditions that can be transmitted to the thin-walled microvessels of the aged brain causing acute microvascular injury and small hemorrhages. Therefore, we propose that age-related impairment of autoregulatory protection may also contribute to the increased prevalence of cerebral microbleeds in elderly hypertensive patients.[185] Because accumulating evidence supports a causal role of cerebral microbleeds for cognitive decline, future studies should elucidate the link between changes in 20-HETE/TRPC6 pathway and incidence of cerebral microbleeds in aging. Finally, hypertension in the elderly is a recognized risk factor for Alzheimer's disease.[142] Because there is increasing evidence that BBB disruption contributes to the development of the disease in mouse models,[166] future studies are warranted to elucidate the role of age-related autoregulatory dysfunction and exacerbation of hypertension-induced microvascular injury in the pathogenesis of Alzheimer's disease in elderly patients as well.

II.6. SUMMARY OF NOVEL FINDINGS OF PART II.

The novel findings of these studies are:

1) in cerebral arteries of young hypertensive mice there is an enhanced myogenic- and flow-induced constriction of cerebral arteries,

2) the up-regulation of 20-HETE/TRPC6 pathway is responsible for this adaptation.

3) By adapting to hypertensive condition cerebral arteries of young mice are able to and maintain an enhanced autoregulation of CBF.

4) In cerebral arteries of aged hypertensive mice there is an impaired myogenic- and flow-induced constriction of cerebral arteries.

5) The autoregulatory adaptation is lost in aged hypertensive animals.

6) In aged hypertensive mice there is exacerbated BBB disruption.

7) In aged hypertensive mice there is capillary rarefaction in cerebral tissue.

8) In aged hypertensive mice there is increased neuroinflammation, which likely

9) contributes to learning decline.

III. PEER-REVIEWED PUBLICATIONS OF THE AUTHOR (IF: 41.336)

The thesis is based on the following publications:

1. **Toth P**, Rozsa B, Springo Z, Doczi T, Koller A. Isolated human and rat cerebral arteries constrict to increases in flow. Role of 20-HETE and TXA2 receptors. J Cereb Blood Flow Metab. (10):2096-105. 2011 ***(IF:5.008)***

2. Koller A. and **Toth P**. Contribution of flow-dependent vasomotor mechanism to the autoregulation of cerebral blood flow. J Vasc Res. 49(5):375-89. 2012 ***(IF:2.65)***

3. **Toth P**, Tucsek Z, Sosnowska D, Gautam T, Mitschelen M, Tarantini S, Deak F, Koller A, Sonntag WE, Csiszar A, Ungvari Z. Age-related autoregulatory dysfunction and exacerbation of microvascular injury in mice. 2013 submitted

Other publications:

4. **Toth P**, Koller A, Pusch G, Bosnyak E, Szapary L, Komoly S, Marko L, Nagy J, Wittmann I. Microalbuminuria, indicated by total versus immunoreactive urinary albumins in acute ischemic stroke patients. J Stroke Cerebrovasc Dis. 20(6):510-516. 2011 ***(IF: 1.680)***

5. **Toth P**, Csiszar A, Sosnowska D, Tucsek Z, Cseplo P, Springo Z, Tarantini S, Sonntag WE, Ungvari Z, Koller A. Treatment with the cytochrome P450 ω-hydroxylase inhibitor HET0016 attenuates cerebrovascular inflammation, oxidative stress and improves vasomotor function in spontaneously hypertensive rats. Br J Pharmacol. 2012 *in press* ***(IF:4.409)***

6. Bailey-Downs LC, Mitschelen M, Sosnowska D, **Toth P**, Pinto JT, Ballabh P, Valcarcel-Ares MN, Farley J, Koller A, Henthorn JC, Bass C, Sonntag WE, Ungvari Z, Csiszar A. Liver-specific knockdown of IGF-1 decreases vascular oxidative stress resistance by impairing the Nrf2-dependent antioxidant response: A novel model of vascular aging. J Gerontol A Biol Sci Med Sci. 67(4):313-29. 2012 ***(IF:4.598)***

7. Bailey-Downs LC, Sosnowska D, **Toth P**, Mitschelen M, Gautam T, Henthorn J, Ballabh P, Koller A, Farley J, Sonntag WE, Csiszar A, Ungvari Z. Growth hormone and IGF-1 deficiency exacerbates high fat diet-induced endothelial impairment in obese Lewis dwarf rats: implications for vascular aging. J Gerontol A Biol Sci Med Sci. 67(6):553-64. 2012 ***(IF:4.598)***

8. Csiszar A, Sosnowska D, Tucsek Z, Gautam T, **Toth P**, Losonczy G, Colman RJ, Weindruch R, Anderson RM, Sonntag WE, Ungvari Z. Circulating factors induced by caloric restriction in the nonhuman primate Macaca Mulatta activate angiogenic processes in endothelial cells. J Gerontol A Biol Sci Med Sci. 2012 Aug 17. *In press* ***(IF: 4.598)***

9. Tucsek Z, Gautam T, Sonntag WE, **Toth P**, Saito H, Salomao R, Szabo Cs, Csiszar A, Ungvari Z. Aging exacerbates microvascular endothelial damage induced by circulating factors present in the serum of septic patients. J Gerontol A Biol Sci Med Sci. 2012 *in press* **(*IF:4.598)***

10. Bailey-Downs LC, Tucsek Z, **Toth P**, Sosnowska D, Gautam T, Sonntag WE, Csiszar A, Ungvari Z. Aging exacerbates obesity-induced oxidative stress and inflammation in perivascular adipose tissue in mice: a paracrine mechanism contributing to vascular redox dysregulation and inflammation. J. Gerontol A Biol Sci Med Sci. 2012 *in press* ***(IF:4.598)***

11. Ungvari Z, Tucsek Z, Sosnowska D, **Toth P**, Gautam T, Podlutsky A, Csiszar A, Losonczy G, Valcarcel-Ares NM, Sonntag WE, Csiszar A. Aging-induced dysregulation of Dicer1-dependent microRNA expression impairs angiogenic capacity of rat cerebromicrovascular endothelial cells. J. Gerontol A Biol Sci Med Sci. 2012 *in press* ***(IF:4.598)***

Abstracts in peer-reviewed journals

1. Degrell P, Molnar L, Pollak E, **Toth P**, Molnar GA, Nagy J, Wittmann I. Ultrastructural localization and pathophysiological importance of the IgA deposits of the mesangial matrix in IgA nephropathy. Act Phys Hun 93(2-3): 165-166. 2006.

2. Degrell P, Kellermayer M, Berta G, **Toth P**, Fincsur A, Gyomorei Cs, Molnar GA, Nagy J, Wittmann Exact localization of fibrinogen-fibrin using laser scanning confocal microscopy in various renal disease and its importance. Act Phys Hun 94(4): 341. 2007.

3. **Toth P**, Halmai R, Marko L, Bosnyak E, Toth M, Bagoly E, Szapary L, Wittmann I, Nagy J, Koller A, Komoly S. Manifestation of systemic vascular disease: microalbuminuria and renal dysfunction in acute stroke. J Vasc Res. 45 (suppl 2) 119; 2008.

4. **Toth P**, Toth J, Marki A, Racz A, Veresh Z, Koller A. In vitro methods to investigate the vasomotor activity of microvessels. J Vasc Res. 45 (suppl 2) 114; 2008.

5. Halmai R, Fesus G, **Toth P**, Koller A, Wittmann I. Water-soluble components of cigarette smoke elicits endothelium independent relaxation of rat renal arteries. J Vasc Res. 45 (suppl 2) 118; 2008.

6. Banga P, Racz A, Veresh Z, **Toth P**, Marki A, Koller A. Temperature substantially modulates the basal tone of arterioles. J Vasc Res. 45(suppl 2) 109; 2008.

7. **Toth P**, Halmai R, Marko L, Bosnyak E, Toth M, Bagoly E, Szapary L, Wittmann I, Nagy J, Koller A, Komoly S. Evaulation of kidney function and microalbuminuria in patients with acute stroke. Act Phys Hun 96(1): 140-140. 2009.

8. **Toth P**, Koller A, Marko L, Halmai R, Bosnyak E, Szapary L, Komoly S, Nagy J, Wittmann I. Correlation between acute stroke and microalbuminuria. Potential role of underlying systemic microvascular endothelial disease. *FASEB J.* 23:613.9. 2009.

9. **Toth P**, Vamos Z, Rozsa B, Hamar J, Komoly S, Koller S. Flow/Shear-Stress induced constrictions of rat middle cerebral artery. „Works and views in endothelium dependent vasodilation". Iasi, Romania, may 13-14. 2009.

10. **Toth P**, Koller A, Marko L, Halmai R, Bosnyak E, Szapary L, Komoly S, Nagy J, Wittmann I. HPLC is more sensitive to assess urinary albumin than nephelometry in acute stroke patients. *FASEB J.* 23:613.10. 2009.

11. Halmai R, Szijjártó I, Brasnyó P, Fésüs G, **Toth P**, Pusch G, Koller A, Wittmann I. Water extracts of cigarette smoke elicit smooth muscle dependent relaxation of rat renal arteries. Water extracts of cigarette smoke elicit smooth muscle dependent relaxation of rat renal arteries. *FASEB J.* 23:804.23. 2009.

12. **Toth P**, Vamos Z, Rozsa B, Tekus E, Cseplo P, Hamar J, Komoly S, Koller A. Increases in flow/shear stress elicit constrictions of small cerebral arteries. Act Phys Hun 97(1): 144-145. 2010.

13. Springo Z, **Toth P**, Komoly S and Koller A (2010). Flow/shear stress-induced responses are opposite in cerebral arteries of different locations. *Frontiers in Neuroscience. Conference Abstract: IBRO International Workshop 2010*. doi: 10.3389/conf.fnins.2010.10.00130

14. **Toth P**, Vamos Z, Springo Z, Komoly S, Doczi T, Koller A. Flow/shear stress-induced constriction of rat middle cerebral artery. *FASEB J*. 976.1 2010

15. Marki A, Gara A, Veresh Z, Seress L, **Toth P**, Koller A. Role of endothelial surface layer in mediation of flow-induce dilation of isolated arterioles. *FASEB J*. 975.15. 2010

16. Koller A, **Toth P**, Rozsa B, Cseplo P, Hamar J, Vamos Z. Aging-induced changes in angiotensin II-induced contractions and tachyphylaxis of isolated carotid arteries. *FASEB J*. 775.1. 2010.

17. Vamos Z, Cseplo P, Koller H, Degrell P, Hamar J, **Toth P**, Koller A. Functional availability of vascular angiotensin type 1 (AT1) receptors is altered by aging *FASEB J.* 25:635.2. 2011.

18. Bailey-Downs LC, Mitschelen M, Sosnowska D, Valcarcel-Ares NM, **Toth P**, Koller A, Gautam T, Pinto J, Henthorn J, Sonntag WE, Csiszar A, Ungvari Z. Liver-specific knockdown of IGF-1 decreases vascular oxidative stress resistance by impairing the Nrf2-dependent antioxidant response *FASEB J. 25:1093.6. 2011*

19. **Toth P**, Doczi T, Koller A. Both human and rat cerebral arteries constrict to increase in intraluminal flow. A novel aspect of the autoregulation of cerebral blood flow *FASEB J.*25:815.2. 2011

20. **Toth, P**, Csiszar A, Sosnowska D, Sonntag WE, Ungvari Z, Koller A. In hypertension CYP450A metabolite 20-HETE exacerbates flow-induced arteriolar constriction and promotes cerebrovascular inflammation. FASEB J. 26:853.24. 2012

21. **Toth P**, Tucsek Z, Baley-Downs L, Sosnowska D, Gautam T, Sonntag WE, Ungvari Z, Csiszar A. High fat diet-induced obesity promotes cerebrovascular autoregulatory dysfunction in aged mice. FASEB J. 26:685.30. 2012

22. Tucsek Z, Gautam T, Sonntag WE, **Toth P**, Csiszar A, Saito h, Szabo C, Ungvari Z. Aging exacerbates microvascular endothelial damage induced by inflammatory factors present in the circulation during sepsis. FASEB J. 2012 26:1058.11.

23. Bailey-Downs LC, Sosnowska D, **Toth P**, Mitschelen M, Gautam T, Henthorn J, Ballabh P, Koller A, Farley J, Sonntag WE, Ungvari Z, Csiszar A. Growth hormone and IGF-1 deficiency exacerbate high fat diet-induced endothelial impairment in obese Lewis dwarf rats: implications for vascular aging *FASEB J* March 29, 2012 26:1057.12

24. Springo Z, **Toth P**, Cseplo P, Szijjarto G, Koller A. The nature and mediation of flow-induced responses of cerebral arteries depends on the origin of vessels. Cardiovascular Research 93: p. S33. 2012

IV. ACKNOWLEDGEMENT

I would like to express my gratefulness to my mentor, Prof. Akos Koller, who opened the world to me and thought me the critical way of thinking (not only in science); and for his continuous support not only as a supervisor but as a friend, as well.

I'd like to thank Dr. Zoltan Ungvari and Dr. Anna Csiszar for being my "second" mentors, for showing me how to choose amongst methodological approaches in order to translate ideas and associations into scientific projects, and for always supporting me to follow my own way in science.

I thank Prof. Samuel Komoly for his help in the initiation of my medical research, and Prof. Tamas Doczi for contributing to my work.

I also would like to express my appreciation to the late Prof. Gabor Kaley, because he made it possible for me to perform my studies at New York Medical College, and because I had the opportunity to get to know him, a legendary person of vascular research. Also, I thank Prof. William E. Sonntag for supporting my research at the University of Oklahoma Health Sciences Center.

I am also grateful to all my colleagues and co-workers in Pecs (Dr. Zoltan Vamos, Dr. Zsolt Springo, Dr. Bernadett Rozsa, Zsuzsanna Dalma Szommer), New York (Dr. Attila Feher, Dr. Nazar Labinsky, Dr. John G. Edwards, Jamie Matthews) and Oklahoma City (Dr. Zsuzsanna Tucsek, Dr. Danuta Sosnowska, Dr. Lora Baley-Downs, Tripti Gautam, Matthew Mitschelen, Julie Farley, Judy Kranz) for helping me in my research projects and contributing to their success.

Finally, I would like to thank to my family: to my parents, who thought me humanity, honor and humbleness; to my brothers and close friends for accepting and loving me in the way I am; and last but most to my wife, Niki, who completes my life and makes me a better person every day.

This work was supported by grants from the American Heart Association (to PT, AC, ZU and AK), the American Federation for Aging Research (to AC), the Oklahoma Center for the Advancement of Science and Technology (to AC, ZU, WES), the NIH (AC, ZU, WES and AK), the Ellison Medical Foundation (to WES), the Hungarian National Science Research Fund OTKA, the MHT (Hungary) (AK) and the Nemzeti Fejlesztési Ügynökség (TÁMOP AK).

V. REFERENCES

1. Schaller B, Graf R. Different compartments of intracranial pressure and its relationship to cerebral blood flow. *J Trauma*. 2005;59:1521-1531
2. Attwell D, Buchan AM, Charpak S, Lauritzen M, Macvicar BA, Newman EA. Glial and neuronal control of brain blood flow. *Nature*. 2010;468:232-243
3. Betz E. Cerebral blood flow: Its measurement and regulation. *Physiol Rev*. 1972;52:595-630
4. Harder DR, Gebremedhin D, Narayanan J, Jefcoat C, Falck JR, Campbell WB, Roman R. Formation and action of a p-450 4a metabolite of arachidonic acid in cat cerebral microvessels. *Am J Physiol*. 1994;266:H2098-2107
5. Harper AM. Autoregulation of cerebral blood flow: Influence of the arterial blood pressure on the blood flow through the cerebral cortex. *J Neurol Neurosurg Psychiatry*. 1966;29:398-403
6. Kontos HA. Regulation of the cerebral circulation. *Annu Rev Physiol*. 1981;43:397-407
7. Lassen NA. Cerebral blood flow and oxygen consumption in man. *Physiol Rev*. 1959;39:183-238
8. Lassen NA. Control of cerebral circulation in health and disease. *Circ Res*. 1974;34:749-760
9. McHedlishvili G. Physiological mechanisms controlling cerebral blood flow. *Stroke*. 1980;11:240-248
10. McHedlishvili GI, Mitagvaria NP, Ormotsadze LG. Vascular mechanisms controlling a constant blood supply to the brain ("autoregulation"). *Stroke*. 1973;4:742-750
11. van Beek AH, Claassen JA, Rikkert MG, Jansen RW. Cerebral autoregulation: An overview of current concepts and methodology with special focus on the elderly. *J Cereb Blood Flow Metab*. 2008;28:1071-1085
12. Rosenblum WI, Shimizu T, Nelson GH. Endothelium-dependent effects of substance p and calcitonin gene-related peptide on mouse pial arterioles. *Stroke*. 1993;24:1043-1047; discussion 1047-1048
13. Rosenblum WI, Wei EP, Kontos HA. Dilation of rat brain arterioles by hypercapnia in vivo can occur even after blockade of guanylate cyclase by odq. *Eur J Pharmacol*. 2002;448:201-206
14. Kovach AG, Dora E, Szedlacsek S, Koller A. Effect of the organic calcium antagonist d-600 on cerebrocortical vascular and redox responses evoked by adenosine, anoxia, and epilepsy. *J Cereb Blood Flow Metab*. 1983;3:51-61
15. Dora E, Koller A, Kovach AG. Effect of topical adenosine deaminase treatment on the functional hyperemic and hypoxic responses of cerebrocortical microcirculation. *J Cereb Blood Flow Metab*. 1984;4:447-457
16. Faraci FM, Baumbach GL, Heistad DD. Myogenic mechanisms in the cerebral circulation. *J Hypertens Suppl*. 1989;7:S61-64; discussion S65
17. Iadecola C, Yang G, Ebner TJ, Chen G. Local and propagated vascular responses evoked by focal synaptic activity in cerebellar cortex. *J Neurophysiol*. 1997;78:651-659
18. Kontos HA, Wei EP, Navari RM, Levasseur JE, Rosenblum WI, Patterson JL, Jr. Responses of cerebral arteries and arterioles to acute hypotension and hypertension. *Am J Physiol*. 1978;234:H371-383
19. Lassen NA, Christensen MS. Physiology of cerebral blood flow. *Br J Anaesth*. 1976;48:719-734
20. Cipolla MJ, Gokina NI, Osol G. Pressure-induced actin polymerization in vascular smooth muscle as a mechanism underlying myogenic behavior. *Faseb J*. 2002;16:72-76
21. Osol G, Brekke JF, McElroy-Yaggy K, Gokina NI. Myogenic tone, reactivity, and forced dilatation: A three-phase model of in vitro arterial myogenic behavior. *Am J Physiol Heart Circ Physiol*. 2002;283:H2260-2267
22. Osol G, Halpern W. Myogenic properties of cerebral blood vessels from normotensive and hypertensive rats. *Am J Physiol*. 1985;249:H914-921
23. Toth P, Rozsa B, Springo Z, Doczi T, Koller A. Isolated human and rat cerebral arteries constrict to increases in flow: Role of 20-hete and tp receptors. *J Cereb Blood Flow Metab*. 2011;31:2096-2105

24. Wallis SJ, Firth J, Dunn WR. Pressure-induced myogenic responses in human isolated cerebral resistance arteries. *Stroke*. 1996;27:2287-2290; discussion 2291
25. Schaller B, Graf R. Different compartments of intracranial pressure and its relationship to cerebral blood flow. *J Trauma*. 2005;59:1521-1531
26. Lucas SJ, Tzeng YC, Galvin SD, Thomas KN, Ogoh S, Ainslie PN. Influence of changes in blood pressure on cerebral perfusion and oxygenation. *Hypertension*. 2010;55:698-705
27. Rosenblum WI. Autoregulatory plateau: Does it exist? *J Cereb Blood Flow Metab*. 1995;15:174-177
28. Peterson EC, Wang Z, Britz G. Regulation of cerebral blood flow. *Int J Vasc Med*. 2011;2011:823525
29. Rosenblum WI. Is the edrf in the cerebral circulation no? Its release by shear and the dangers in interpreting the effects of nos inhibitors. *Keio J Med*. 1998;47:142-149
30. Pohl U, de Wit C. A unique role of no in the control of blood flow. *News Physiol Sci*. 1999;14:74-80
31. Pohl U, Herlan K, Huang A, Bassenge E. Edrf-mediated shear-induced dilation opposes myogenic vasoconstriction in small rabbit arteries. *Am J Physiol*. 1991;261:H2016-2023
32. Sun D, Huang A, Koller A, Kaley G. Flow-dependent dilation and myogenic constriction interact to establish the resistance of skeletal muscle arterioles. *Microcirculation*. 1995;2:289-295
33. Ungvari Z, Koller A. Selected contribution: No released to flow reduces myogenic tone of skeletal muscle arterioles by decreasing smooth muscle ca(2+) sensitivity. *J Appl Physiol*. 2001;91:522-527; discussion 504-525
34. Faraci FM, Heistad DD. Regulation of large cerebral arteries and cerebral microvascular pressure. *Circ Res*. 1990;66:8-17
35. Harper SL, Bohlen HG, Rubin MJ. Arterial and microvascular contributions to cerebral cortical autoregulation in rats. *Am J Physiol*. 1984;246:H17-24
36. Stromberg DD, Fox JR. Pressures in the pial arterial microcirculation of the cat during changes in systemic arterial blood pressure. *Circ Res*. 1972;31:229-239
37. Baumbach GL, Heistad DD. Regional, segmental, and temporal heterogeneity of cerebral vascular autoregulation. *Ann Biomed Eng*. 1985;13:303-310
38. Baumbach GL, Heistad DD. Heterogeneity of brain blood flow and permeability during acute hypertension. *Am J Physiol*. 1985;249:H629-637
39. Mueller SM, Heistad DD, Marcus ML. Total and regional cerebral blood flow during hypotension, hypertension, and hypocapnia. Effect of sympathetic denervation in dogs. *Circ Res*. 1977;41:350-356
40. Rozet I, Vavilala MS, Lindley AM, Visco E, Treggiari M, Lam AM. Cerebral autoregulation and co2 reactivity in anterior and posterior cerebral circulation during sevoflurane anesthesia. *Anesth Analg*. 2006;102:560-564
41. Willie CK, Colino FL, Bailey DM, Tzeng YC, Binsted G, Jones LW, Haykowsky MJ, Bellapart J, Ogoh S, Smith KJ, Smirl JD, Day TA, Lucas SJ, Eller LK, Ainslie PN. Utility of transcranial doppler ultrasound for the integrative assessment of cerebrovascular function. *J Neurosci Methods*. 2011;196:221-237
42. Faraci FM, Mayhan WG, Heistad DD. Segmental vascular responses to acute hypertension in cerebrum and brain stem. *Am J Physiol*. 1987;252:H738-742
43. Mayhan WG, Faraci FM, Heistad DD. Disruption of the blood-brain barrier in cerebrum and brain stem during acute hypertension. *Am J Physiol*. 1986;251:H1171-1175
44. Cipolla MJ. *The cerebral circulation*. San Rafael (CA); 2009.
45. Ayata C, Dunn AK, Gursoy OY, Huang Z, Boas DA, Moskowitz MA. Laser speckle flowmetry for the study of cerebrovascular physiology in normal and ischemic mouse cortex. *J Cereb Blood Flow Metab*. 2004;24:744-755
46. Bellapart J, Fraser JF. Transcranial doppler assessment of cerebral autoregulation. *Ultrasound Med Biol*. 2009;35:883-893
47. Faraci FM, Heistad DD. Regulation of the cerebral circulation: Role of endothelium and potassium channels. *Physiol Rev*. 1998;78:53-97

48. Lunn V, Fog M. The reaction of the pial arteries to some cholin-like and adrenalin-like substances. *J Neurol Psychiatry*. 1939;2:223-230
49. MacKenzie ET, Farrar JK, Fitch W, Graham DI, Gregory PC, Harper AM. Effects of hemorrhagic hypotension on the cerebral circulation. I. Cerebral blood flow and pial arteriolar caliber. *Stroke*. 1979;10:711-718
50. MacKenzie ET, Strandgaard S, Graham DI, Jones JV, Harper AM, Farrar JK. Effects of acutely induced hypertension in cats on pial arteriolar caliber, local cerebral blood flow, and the blood-brain barrier. *Circ Res*. 1976;39:33-41
51. Magun JG. The effect of pharmacologically increased blood pressure on brain circulation. Angiographic investigation of arterial diameter and blood flow in patients with normal and pathological angiograms. *Z Neurol*. 1973;204:107-134
52. Zaharchuk G, Mandeville JB, Bogdanov AA, Jr., Weissleder R, Rosen BR, Marota JJ. Cerebrovascular dynamics of autoregulation and hypoperfusion. An mri study of cbf and changes in total and microvascular cerebral blood volume during hemorrhagic hypotension. *Stroke*. 1999;30:2197-2204; discussion 2204-2195
53. Bayliss WM. On the local reactions of the arterial wall to changes of internal pressure. *J Physiol*. 1902;28:220-231
54. Fog M. The relationship between the blood pressure and the tonic regulation of the pial arteries. *J Neurol Psychiatry*. 1938;1:187-197
55. Forbes HS. Regulation of the cerebral vessels; new aspects. *AMA Arch Neurol Psychiatry*. 1958;80:689-695
56. Vinall PE, Simeone FA. Cerebral autoregulation: An in vitro study. *Stroke*. 1981;12:640-642
57. Koller A, Bagi Z. On the role of mechanosensitive mechanisms eliciting reactive hyperemia. *Am J Physiol Heart Circ Physiol*. 2002;283:H2250-2259
58. Koller A, Sun D, Huang A, Kaley G. Corelease of nitric oxide and prostaglandins mediates flow-dependent dilation of rat gracilis muscle arterioles. *Am J Physiol*. 1994;267:H326-332
59. Koller A, Sun D, Kaley G. Role of shear stress and endothelial prostaglandins in flow- and viscosity-induced dilation of arterioles in vitro. *Circ Res*. 1993;72:1276-1284
60. de Wit C, Jahrbeck B, Schafer C, Bolz SS, Pohl U. Nitric oxide opposes myogenic pressure responses predominantly in large arterioles in vivo. *Hypertension*. 1998;31:787-794
61. Bohlen HG, Harper SL. Evidence of myogenic vascular control in the rat cerebral cortex. *Circ Res*. 1984;55:554-559
62. Meininger GA, Mack CA, Fehr KL, Bohlen HG. Myogenic vasoregulation overrides local metabolic control in resting rat skeletal muscle. *Circ Res*. 1987;60:861-870
63. Paulson OB, Strandgaard S, Edvinsson L. Cerebral autoregulation. *Cerebrovasc Brain Metab Rev*. 1990;2:161-192
64. Korzick DH, Laughlin MH, Bowles DK. Alterations in pkc signaling underlie enhanced myogenic tone in exercise-trained porcine coronary resistance arteries. *J Appl Physiol*. 2004;96:1425-1432
65. Ping P, Johnson PC. Role of myogenic response in enhancing autoregulation of flow during sympathetic nerve stimulation. *Am J Physiol*. 1992;263:H1177-1184
66. Cole WC, Welsh DG. Role of myosin light chain kinase and myosin light chain phosphatase in the resistance arterial myogenic response to intravascular pressure. *Arch Biochem Biophys*. 2011;510:160-173
67. Hill MA, Davis MJ, Meininger GA, Potocnik SJ, Murphy TV. Arteriolar myogenic signalling mechanisms: Implications for local vascular function. *Clin Hemorheol Microcirc*. 2006;34:67-79
68. Schubert R, Lidington D, Bolz SS. The emerging role of ca2+ sensitivity regulation in promoting myogenic vasoconstriction. *Cardiovasc Res*. 2008;77:8-18
69. Harder DR, Narayanan J, Gebremedhin D. Pressure-induced myogenic tone and role of 20-hete in mediating autoregulation of cerebral blood flow. *American journal of physiology. Heart and circulatory physiology*. 2011;300:H1557-1565
70. Somlyo AP, Somlyo AV. Ca2+ sensitivity of smooth muscle and nonmuscle myosin ii: Modulated by g proteins, kinases, and myosin phosphatase. *Physiol Rev*. 2003;83:1325-1358

71. Johnson PC. The myogenic response in the microcirculation and its interaction with other control systems. *J Hypertens Suppl*. 1989;7:S33-39; discussion S40
72. D'Angelo G, Mogford JE, Davis GE, Davis MJ, Meininger GA. Integrin-mediated reduction in vascular smooth muscle [ca2+]i induced by rgd-containing peptide. *Am J Physiol*. 1997;272:H2065-2070
73. Davis MJ, Donovitz JA, Hood JD. Stretch-activated single-channel and whole cell currents in vascular smooth muscle cells. *Am J Physiol*. 1992;262:C1083-1088
74. Lucchesi PA, Sabri A, Belmadani S, Matrougui K. Involvement of metalloproteinases 2/9 in epidermal growth factor receptor transactivation in pressure-induced myogenic tone in mouse mesenteric resistance arteries. *Circulation*. 2004;110:3587-3593
75. Martinez-Lemus LA, Crow T, Davis MJ, Meininger GA. Alphavbeta3- and alpha5beta1-integrin blockade inhibits myogenic constriction of skeletal muscle resistance arterioles. *American journal of physiology. Heart and circulatory physiology*. 2005;289:H322-329
76. Knot HJ, Nelson MT. Regulation of arterial diameter and wall [ca2+] in cerebral arteries of rat by membrane potential and intravascular pressure. *J Physiol*. 1998;508 (Pt 1):199-209
77. Welsh DG, Nelson MT, Eckman DM, Brayden JE. Swelling-activated cation channels mediate depolarization of rat cerebrovascular smooth muscle by hyposmolarity and intravascular pressure. *J Physiol*. 2000;527 Pt 1:139-148
78. Welsh DG, Morielli AD, Nelson MT, Brayden JE. Transient receptor potential channels regulate myogenic tone of resistance arteries. *Circ Res*. 2002;90:248-250
79. Earley S, Waldron BJ, Brayden JE. Critical role for transient receptor potential channel trpm4 in myogenic constriction of cerebral arteries. *Circ Res*. 2004;95:922-929
80. Drummond HA, Grifoni SC, Jernigan NL. A new trick for an old dogma: Enac proteins as mechanotransducers in vascular smooth muscle. *Physiology (Bethesda)*. 2008;23:23-31
81. Dopico AM, Kirber MT, Singer JJ, Walsh JV, Jr. Membrane stretch directly activates large conductance ca(2+)-activated k+ channels in mesenteric artery smooth muscle cells. *Am J Hypertens*. 1994;7:82-89
82. Nelson MT, Conway MA, Knot HJ, Brayden JE. Chloride channel blockers inhibit myogenic tone in rat cerebral arteries. *J Physiol*. 1997;502 (Pt 2):259-264
83. Knot HJ, Nelson MT. Regulation of membrane potential and diameter by voltage-dependent k+ channels in rabbit myogenic cerebral arteries. *Am J Physiol*. 1995;269:H348-355
84. McCarron JG, Crichton CA, Langton PD, MacKenzie A, Smith GL. Myogenic contraction by modulation of voltage-dependent calcium currents in isolated rat cerebral arteries. *J Physiol*. 1997;498 (Pt 2):371-379
85. Moosmang S, Schulla V, Welling A, Feil R, Feil S, Wegener JW, Hofmann F, Klugbauer N. Dominant role of smooth muscle l-type calcium channel cav1.2 for blood pressure regulation. *Embo J*. 2003;22:6027-6034
86. Moosmang S, Haider N, Bruderl B, Welling A, Hofmann F. Antihypertensive effects of the putative t-type calcium channel antagonist mibefradil are mediated by the l-type calcium channel cav1.2. *Circ Res*. 2006;98:105-110
87. Watanabe J, Horiguchi S, Karibe A, Keitoku M, Takeuchi M, Satoh S, Takishima T, Shirato K. Effects of ryanodine on development of myogenic response in rat small skeletal muscle arteries. *Cardiovasc Res*. 1994;28:480-484
88. Davis MJ, Hill MA. Signaling mechanisms underlying the vascular myogenic response. *Physiol Rev*. 1999;79:387-423
89. Schubert R, Mulvany MJ. The myogenic response: Established facts and attractive hypotheses. *Clin Sci (Lond)*. 1999;96:313-326
90. Hill MA, Zou H, Potocnik SJ, Meininger GA, Davis MJ. Invited review: Arteriolar smooth muscle mechanotransduction: Ca(2+) signaling pathways underlying myogenic reactivity. *J Appl Physiol*. 2001;91:973-983
91. Pfitzer G. Invited review: Regulation of myosin phosphorylation in smooth muscle. *J Appl Physiol*. 2001;91:497-503

92. Lagaud G, Gaudreault N, Moore ED, Van Breemen C, Laher I. Pressure-dependent myogenic constriction of cerebral arteries occurs independently of voltage-dependent activation. *American journal of physiology. Heart and circulatory physiology*. 2002;283:H2187-2195
93. Narayanan J, Imig M, Roman RJ, Harder DR. Pressurization of isolated renal arteries increases inositol trisphosphate and diacylglycerol. *Am J Physiol*. 1994;266:H1840-1845
94. Gebremedhin D, Lange AR, Lowry TF, Taheri MR, Birks EK, Hudetz AG, Narayanan J, Falck JR, Okamoto H, Roman RJ, Nithipatikom K, Campbell WB, Harder DR. Production of 20-hete and its role in autoregulation of cerebral blood flow. *Circ Res*. 2000;87:60-65
95. Gebremedhin D, Lange AR, Narayanan J, Aebly MR, Jacobs ER, Harder DR. Cat cerebral arterial smooth muscle cells express cytochrome p450 4a2 enzyme and produce the vasoconstrictor 20-hete which enhances l-type ca2+ current. *J Physiol*. 1998;507 (Pt 3):771-781
96. Frisbee JC, Roman RJ, Falck JR, Krishna UM, Lombard JH. 20-hete contributes to myogenic activation of skeletal muscle resistance arteries in brown norway and sprague-dawley rats. *Microcirculation*. 2001;8:45-55
97. Lange A, Gebremedhin D, Narayanan J, Harder D. 20-hydroxyeicosatetraenoic acid-induced vasoconstriction and inhibition of potassium current in cerebral vascular smooth muscle is dependent on activation of protein kinase c. *J Biol Chem*. 1997;272:27345-27352
98. Laher I, Bevan JA. Protein kinase c activation selectively augments a stretch-induced, calcium-dependent tone in vascular smooth muscle. *J Pharmacol Exp Ther*. 1987;242:566-572
99. Garcia-Roldan JL, Bevan JA. Flow-induced constriction and dilation of cerebral resistance arteries. *Circ Res*. 1990;66:1445-1448
100. Garcia-Roldan JL, Bevan JA. Augmentation of endothelium-independent flow constriction in pial arteries at high intravascular pressures. *Hypertension*. 1991;17:870-874
101. Ngai AC, Winn HR. Modulation of cerebral arteriolar diameter by intraluminal flow and pressure. *Circ Res*. 1995;77:832-840
102. Shimoda LA, Norins NA, Jeutter DC, Madden JA. Flow-induced responses in piglet isolated cerebral arteries. *Pediatr Res*. 1996;39:574-583
103. Shimoda LA, Norins NA, Madden JA. Responses to pulsatile flow in piglet isolated cerebral arteries. *Pediatr Res*. 1998;43:514-520
104. Thorin-Trescases N, Bevan JA. High levels of myogenic tone antagonize the dilator response to flow of small rabbit cerebral arteries. *Stroke*. 1998;29:1194-1200; discussion 1200-1191
105. Bryan RM, Jr., Marrelli SP, Steenberg ML, Schildmeyer LA, Johnson TD. Effects of luminal shear stress on cerebral arteries and arterioles. *Am J Physiol Heart Circ Physiol*. 2001;280:H2011-2022
106. Madden JA, Christman NJ. Integrin signaling, free radicals, and tyrosine kinase mediate flow constriction in isolated cerebral arteries. *Am J Physiol*. 1999;277:H2264-2271
107. Gaw AJ, Bevan JA. Flow-induced relaxation of the rabbit middle cerebral artery is composed of both endothelium-dependent and -independent components. *Stroke*. 1993;24:105-109; discussion 109-110
108. Drouin A, Thorin E. Flow-induced dilation is mediated by akt-dependent activation of endothelial nitric oxide synthase-derived hydrogen peroxide in mouse cerebral arteries. *Stroke*. 2009;40:1827-1833
109. Drouin A, Bolduc V, Thorin-Trescases N, Belanger E, Fernandes P, Baraghis E, Lesage F, Gillis MA, Villeneuve L, Hamel E, Ferland G, Thorin E. Catechin treatment improves cerebrovascular flow-mediated dilation and learning abilities in atherosclerotic mice. *Am J Physiol Heart Circ Physiol*.300:H1032-1043
110. Sipkema P, van der Linden PJ, Fanton J, Latham RD. Responses to mechanical stimuli of isolated basilar and femoral arteries of the rhesus monkey are different. *Heart Vessels*. 1996;11:18-26
111. Koller A, Seyedi N, Gerritsen ME, Kaley G. Edrf released from microvascular endothelial cells dilates arterioles in vivo. *Am J Physiol*. 1991;261:H128-133

112. Bryan RM, Jr., Steenberg ML, Marrelli SP. Role of endothelium in shear stress-induced constrictions in rat middle cerebral artery. *Stroke*. 2001;32:1394-1400
113. Kim YS, Bogert LW, Immink RV, Harms MP, Colier WN, van Lieshout JJ. Effects of aging on the cerebrovascular orthostatic response. *Neurobiol Aging*. 2011;32:344-353
114. Fujii K, Heistad DD, Faraci FM. Flow-mediated dilatation of the basilar artery in vivo. *Circ Res*. 1991;69:697-705
115. Fujii K, Heistad DD, Faraci FM. Effect of diabetes mellitus on flow-mediated and endothelium-dependent dilatation of the rat basilar artery. *Stroke*. 1992;23:1494-1498
116. Paravicini TM, Miller AA, Drummond GR, Sobey CG. Flow-induced cerebral vasodilatation in vivo involves activation of phosphatidylinositol-3 kinase, nadph-oxidase, and nitric oxide synthase. *J Cereb Blood Flow Metab*. 2006;26:836-845
117. Drouin A, Bolduc V, Thorin-Trescases N, Belanger E, Fernandes P, Baraghis E, Lesage F, Gillis MA, Villeneuve L, Hamel E, Ferland G, Thorin E. Catechin treatment improves cerebrovascular flow-mediated dilation and learning abilities in atherosclerotic mice. *American journal of physiology. Heart and circulatory physiology*. 2011;300:H1032-1043
118. Ward ME, Yan L, Kelly S, Angle MR. Flow modulation of pressure-sensitive tone in rat pial arterioles: Role of the endothelium. *Anesthesiology*. 2000;93:1456-1464
119. Ungvari Z, Pacher P, Kecskemeti V, Koller A. Fluoxetine dilates isolated small cerebral arteries of rats and attenuates constrictions to serotonin, norepinephrine, and a voltage-dependent ca(2+) channel opener. *Stroke*. 1999;30:1949-1954
120. Racz A, Veresh Z, Lotz G, Bagi Z, Koller A. Cyclooxygenase-2 derived thromboxane a(2) and reactive oxygen species mediate flow-induced constrictions of venules in hyperhomocysteinemia. *Atherosclerosis*.208:43-49
121. Fink B, Laude K, McCann L, Doughan A, Harrison DG, Dikalov S. Detection of intracellular superoxide formation in endothelial cells and intact tissues using dihydroethidium and an hplc-based assay. *Am J Physiol Cell Physiol*. 2004;287:C895-902
122. Fujii K, Heistad DD, Faraci FM. Role of the basilar artery in regulation of blood flow to the brain stem in rats. *Stroke*. 1991;22:763-767
123. Bari F, Louis TM, Busija DW. Effects of ischemia on cerebral arteriolar dilation to arterial hypoxia in piglets. *Stroke*. 1998;29:222-227; discussion 227-228
124. Raisis JE, Kindt GW, McGillicuddy JE, Giannotta SL. The effects of primary elevation of cerebral venous pressure on cerebral hemodynamics and intracranial pressure. *J Surg Res*. 1979;26:101-107
125. Gordon GR, Choi HB, Rungta RL, Ellis-Davies GC, MacVicar BA. Brain metabolism dictates the polarity of astrocyte control over arterioles. *Nature*. 2008;456:745-749
126. Golding EM, Robertson CS, Bryan RM, Jr. Comparison of the myogenic response in rat cerebral arteries of different calibers. *Brain Res*. 1998;785:293-298
127. Ellis EF, Nies AS, Oates JA. Cerebral arterial smooth muscle contraction by thromboxane a2. *Stroke*. 1977;8:480-483
128. Dunn KM, Renic M, Flasch AK, Harder DR, Falck J, Roman RJ. Elevated production of 20-hete in the cerebral vasculature contributes to severity of ischemic stroke and oxidative stress in spontaneously hypertensive rats. *Am J Physiol Heart Circ Physiol*. 2008;295:H2455-2465
129. Yu M, Cambj-Sapunar L, Kehl F, Maier KG, Takeuchi K, Miyata N, Ishimoto T, Reddy LM, Falck JR, Gebremedhin D, Harder DR, Roman RJ. Effects of a 20-hete antagonist and agonists on cerebral vascular tone. *Eur J Pharmacol*. 2004;486:297-306
130. Terashvili M, Pratt PF, Gebremedhin D, Narayanan J, Harder DR. Reactive oxygen species cerebral autoregulation in health and disease. *Pediatr Clin North Am*. 2006;53:1029-1037, xi
131. Harder DR, Lange AR, Gebremedhin D, Birks EK, Roman RJ. Cytochrome p450 metabolites of arachidonic acid as intracellular signaling molecules in vascular tissue. *J Vasc Res*. 1997;34:237-243
132. Zou AP, Fleming JT, Falck JR, Jacobs ER, Gebremedhin D, Harder DR, Roman RJ. 20-hete is an endogenous inhibitor of the large-conductance ca(2+)-activated k+ channel in renal arterioles. *Am J Physiol*. 1996;270:R228-237

133. Escalante B, Sessa WC, Falck JR, Yadagiri P, Schwartzman ML. Vasoactivity of 20-hydroxyeicosatetraenoic acid is dependent on metabolism by cyclooxygenase. *J Pharmacol Exp Ther*. 1989;248:229-232
134. Schwartzman ML, Falck JR, Yadagiri P, Escalante B. Metabolism of 20-hydroxyeicosatetraenoic acid by cyclooxygenase. Formation and identification of novel endothelium-dependent vasoconstrictor metabolites. *J Biol Chem*. 1989;264:11658-11662
135. Didion SP, Faraci FM. Effects of nadh and nadph on superoxide levels and cerebral vascular tone. *Am J Physiol Heart Circ Physiol*. 2002;282:H688-695
136. Zhang XM, Ellis EF. Superoxide dismutase decreases mortality, blood pressure, and cerebral blood flow responses induced by acute hypertension in rats. *Stroke*. 1991;22:489-494
137. Lacza Z, Hortobagyi L, Horvath B, Horvath EM, Sandor P, Benyo Z. Additive effect of cyclooxygenase and nitric oxide synthase blockade on the cerebrocortical microcirculation. *Neuroreport*. 2009;20:1027-1031
138. Harder DR, Alkayed NJ, Lange AR, Gebremedhin D, Roman RJ. Functional hyperemia in the brain: Hypothesis for astrocyte-derived vasodilator metabolites. *Stroke*. 1998;29:229-234
139. Wei EP, Kontos HA, Beckman JS. Mechanisms of cerebral vasodilation by superoxide, hydrogen peroxide, and peroxynitrite. *Am J Physiol*. 1996;271:H1262-1266
140. Cosentino F, Sill JC, Katusic ZS. Role of superoxide anions in the mediation of endothelium-dependent contractions. *Hypertension*. 1994;23:229-235
141. Aronow WS, Fleg JL, Pepine CJ, Artinian NT, Bakris G, Brown AS, Ferdinand KC, Forciea MA, Frishman WH, Jaigobin C, Kostis JB, Mancia G, Oparil S, Ortiz E, Reisin E, Rich MW, Schocken DD, Weber MA, Wesley DJ, Harrington RA. Accf/aha 2011 expert consensus document on hypertension in the elderly: A report of the american college of cardiology foundation task force on clinical expert consensus documents. *Circulation*. 2011;123:2434-2506
142. Iadecola C, Park L, Capone C. Threats to the mind: Aging, amyloid, and hypertension. *Stroke*. 2009;40:S40-44
143. Gorelick PB, Scuteri A, Black SE, Decarli C, Greenberg SM, Iadecola C, Launer LJ, Laurent S, Lopez OL, Nyenhuis D, Petersen RC, Schneider JA, Tzourio C, Arnett DK, Bennett DA, Chui HC, Higashida RT, Lindquist R, Nilsson PM, Roman GC, Sellke FW, Seshadri S. Vascular contributions to cognitive impairment and dementia: A statement for healthcare professionals from the american heart association/american stroke association. *Stroke*. 2011;42:2672-2713
144. Brickman AM, Reitz C, Luchsinger JA, Manly JJ, Schupf N, Muraskin J, DeCarli C, Brown TR, Mayeux R. Long-term blood pressure fluctuation and cerebrovascular disease in an elderly cohort. *Arch Neurol*. 2010;67:564-569
145. Reitz C, Tang MX, Manly J, Mayeux R, Luchsinger JA. Hypertension and the risk of mild cognitive impairment. *Arch Neurol*. 2007;64:1734-1740
146. Kuller LH, Lopez OL, Jagust WJ, Becker JT, DeKosky ST, Lyketsos C, Kawas C, Breitner JC, Fitzpatrick A, Dulberg C. Determinants of vascular dementia in the cardiovascular health cognition study. *Neurology*. 2005;64:1548-1552
147. Hachinski V, Iadecola C, Petersen RC, Breteler MM, Nyenhuis DL, Black SE, Powers WJ, DeCarli C, Merino JG, Kalaria RN, Vinters HV, Holtzman DM, Rosenberg GA, Wallin A, Dichgans M, Marler JR, Leblanc GG. National institute of neurological disorders and stroke-canadian stroke network vascular cognitive impairment harmonization standards. *Stroke*. 2006;37:2220-2241
148. Strandgaard S, Jones JV, MacKenzie ET, Harper AM. Upper limit of cerebral blood flow autoregulation in experimental renovascular hypertension in the baboon. *Circ Res*. 1975;37:164-167
149. Harper SL, Bohlen HG. Microvascular adaptation in the cerebral cortex of adult spontaneously hypertensive rats. *Hypertension*. 1984;6:408-419
150. Kontos HA, Wei EP, Raper AJ, Rosenblum WI, Navari RM, Patterson JL, Jr. Role of tissue hypoxia in local regulation of cerebral microcirculation. *Am J Physiol*. 1978;234:H582-591

151. Smeda JS. Cerebral vascular changes associated with hemorrhagic stroke in hypertension. *Can J Physiol Pharmacol*. 1992;70:552-564
152. Tsai JY, Yamamoto T, Fariss R, Hickman F, Pagan-Mercado G. Using smaa-gfp mice to study pericyte coverage of retinal vessels. *Invest Ophthalmol Vis Sci*. 2002;43:12
153. Wakisaka Y, Chu Y, Miller JD, Rosenberg GA, Heistad DD. Spontaneous intracerebral hemorrhage during acute and chronic hypertension in mice. *J Cereb Blood Flow Metab*. 2010;30:56-69
154. Carrie I, Debray M, Bourre JM, Frances H. Age-induced cognitive alterations in of1 mice. *Physiol Behav*. 1999;66:651-656
155. Niwa K, Kazama K, Younkin L, Younkin SG, Carlson GA, Iadecola C. Cerebrovascular autoregulation is profoundly impaired in mice overexpressing amyloid precursor protein. *Am J Physiol Heart Circ Physiol*. 2002;283:H315-323
156. Miyata N, Taniguchi K, Seki T, Ishimoto T, Sato-Watanabe M, Yasuda Y, Doi M, Kametani S, Tomishima Y, Ueki T, Sato M, Kameo K. Het0016, a potent and selective inhibitor of 20-hete synthesizing enzyme. *Br J Pharmacol*. 2001;133:325-329
157. Inoue R, Jensen LJ, Jian Z, Shi J, Hai L, Lurie AI, Henriksen FH, Salomonsson M, Morita H, Kawarabayashi Y, Mori M, Mori Y, Ito Y. Synergistic activation of vascular trpc6 channel by receptor and mechanical stimulation via phospholipase c/diacylglycerol and phospholipase a2/omega-hydroxylase/20-hete pathways. *Circ Res*. 2009;104:1399-1409
158. Brayden JE, Earley S, Nelson MT, Reading S. Transient receptor potential (trp) channels, vascular tone and autoregulation of cerebral blood flow. *Clin Exp Pharmacol Physiol*. 2008;35:1116-1120
159. Toth P, Rozsa B, Springo Z, Doczi T, Koller A. Isolated human and rat cerebral arteries constrict to increases in flow: Role of 20-hete and tp receptors. *J Cereb Blood Flow Metab*. 2011;31:2096-2105
160. Bailey-Downs LC, Mitschelen M, Sosnowska D, Toth P, Pinto JT, Ballabh P, Valcarcel-Ares MN, Farley J, Koller A, Henthorn JC, Bass C, Sonntag WE, Ungvari Z, Csiszar A. Liver-specific knockdown of igf-1 decreases vascular oxidative stress resistance by impairing the nrf2-dependent antioxidant response: A novel model of vascular aging. *J Gerontol Biol Med Sci*. 2012;67:313-329
161. Kaya M, Ahishali B. Assessment of permeability in barrier type of endothelium in brain using tracers: Evans blue, sodium fluorescein, and horseradish peroxidase. *Methods Mol Biol*. 2011;763:369-382
162. Kaya M, Ahishali B. Assessment of permeability in barrier type of endothelium in brain using tracers: Evans blue, sodium fluorescein, and horseradish peroxidase. *Methods Mol Biol*. 2011;763:369-382
163. Winkler EA, Bell RD, Zlokovic BV. Central nervous system pericytes in health and disease. *Nat Neurosci*. 2011;14:1398-1405
164. Warrington JP, Csiszar A, Johnson DA, Herman TS, Ahmad S, Lee YW, Sonntag WE. Cerebral microvascular rarefaction induced by whole brain radiation is reversible by systemic hypoxia in mice. *Am J Physiol Heart Circ Physiol*. 2011;300:H736-744
165. Hof PR, Young WC, Bloom FE, Belichenko PV, Celio MR. *Comparative cytoachitectonic atlas of the c57bl/6 and 129/sv mouse brains*. New York, NY: Elsevier; 2000.
166. Zlokovic BV. The blood-brain barrier in health and chronic neurodegenerative disorders. *Neuron*. 2008;57:178-201
167. Bell RD, Winkler EA, Sagare AP, Singh I, LaRue B, Deane R, Zlokovic BV. Pericytes control key neurovascular functions and neuronal phenotype in the adult brain and during brain aging. *Neuron*. 2010;68:409-427
168. Capone C, Faraco G, Park L, Cao X, Davisson RL, Iadecola C. The cerebrovascular dysfunction induced by slow pressor doses of angiotensin ii precedes the development of hypertension. *Am J Physiol Heart Circ Physiol*. 2011;300:H397-407
169. New DI, Chesser AM, Thuraisingham RC, Yaqoob MM. Cerebral artery responses to pressure and flow in uremic hypertensive and spontaneously hypertensive rats. *Am J Physiol Heart Circ Physiol*. 2003;284:H1212-1216

170. Koller A, Toth P. Contribution of flow-dependent vasomotor mechanisms to the autoregulation of cerebral blood flow. *J Vasc Res*. 2012;49:375-389
171. Inoue R, Jensen LJ, Jian Z, Shi J, Hai L, Lurie AI, Henriksen FH, Salomonsson M, Morita H, Kawarabayashi Y, Mori M, Mori Y, Ito Y. Synergistic activation of vascular trpc6 channel by receptor and mechanical stimulation via phospholipase c/diacylglycerol and phospholipase a2/omega-hydroxylase/20-hete pathways. *Circ Res*. 2009;104:1399-1409
172. Welsh DG, Morielli AD, Nelson MT, Brayden JE. Transient receptor potential channels regulate myogenic tone of resistance arteries. *Circ Res*. 2002;90:248-250
173. Ungvari Z, Csiszar A. The emerging role of igf-1 deficiency in cardiovascular aging: Recent advances. *J Gerontol A Biol Sci Med Sci*. 2012
174. Zhang M, Mao Y, Ramirez SH, Tuma RF, Chabrashvili T. Angiotensin ii induced cerebral microvascular inflammation and increased blood-brain barrier permeability via oxidative stress. *Neuroscience*. 2010;171:852-858
175. Girouard H, Park L, Anrather J, Zhou P, Iadecola C. Angiotensin ii attenuates endothelium-dependent responses in the cerebral microcirculation through nox-2-derived radicals. *Arterioscler Thromb Vasc Biol*. 2006;26:826-832
176. Girouard H, Park L, Anrather J, Zhou P, Iadecola C. Cerebrovascular nitrosative stress mediates neurovascular and endothelial dysfunction induced by angiotensin ii. *Arterioscler Thromb Vasc Biol*. 2007;27:303-309
177. Fernandez-Vizarra P, Lopez-Franco O, Mallavia B, Higuera-Matas A, Lopez-Parra V, Ortiz-Munoz G, Ambrosio E, Egido J, Almeida OF, Gomez-Guerrero C. Immunoglobulin g fc receptor deficiency prevents alzheimer-like pathology and cognitive impairment in mice. *Brain*. 2012;135:2826-2837
178. Kaneko YS, Nakashima A, Mori K, Nagatsu T, Nagatsu I, Ota A. Microglial activation in neuroinflammation: Implications for the etiology of neurodegeneration. *Neurodegener Dis*. 2012;10:100-103
179. Ando H, Zhou J, Macova M, Imboden H, Saavedra JM. Angiotensin ii at1 receptor blockade reverses pathological hypertrophy and inflammation in brain microvessels of spontaneously hypertensive rats. *Stroke*. 2004;35:1726-1731
180. Gao HM, Liu B, Zhang W, Hong JS. Critical role of microglial nadph oxidase-derived free radicals in the in vitro mptp model of parkinson's disease. *Faseb J*. 2003;17:1954-1956
181. Farrall AJ, Wardlaw JM. Blood-brain barrier: Ageing and microvascular disease--systematic review and meta-analysis. *Neurobiol Aging*. 2009;30:337-352
182. PROGRESS.Collaborative.Group. Randomised trial of a perindopril-based blood-pressure-lowering regimen among 6,105 individuals with previous stroke or transient ischaemic attack. *Lancet*. 2001;358:1033-1041
183. Forette F, Seux ML, Staessen JA, Thijs L, Birkenhager WH, Babarskiene MR, Babeanu S, Bossini A, Gil-Extremera B, Girerd X, Laks T, Lilov E, Moisseyev V, Tuomilehto J, Vanhanen H, Webster J, Yodfat Y, Fagard R. Prevention of dementia in randomised double-blind placebo-controlled systolic hypertension in europe (syst-eur) trial. *Lancet*. 1998;352:1347-1351
184. Trenkwalder P. The study on cognition and prognosis in the elderly (scope)--recent analyses. *J Hypertens Suppl*. 2006;24:S107-114
185. Poels MM, Ikram MA, van der Lugt A, Hofman A, Krestin GP, Breteler MM, Vernooij MW. Incidence of cerebral microbleeds in the general population: The rotterdam scan study. *Stroke*. 2011;42:656-661